Chapter 5
Tactile Sensing Technologies

Abstract This chapter presents the state-of the-art of robotic tactile sensing technologies and analyzes the present state of research in the area tactile sensing. Various tactile sensing technologies have been discussed under three categories: (1) transduction methods; (2) structures that generate a signal on touch; and (3) new materials that intrinsically convert mechanical stimulus on touch into usable signals. The tactile sensing technologies are explained along with their merits and demerits. The working principle of various methods have been explained and selected implementations are presented.

Keywords Tactile sensing technologies · Artificial skin · Smart materials · Transducers · Tactile sensor · Tactile sensing array · CMOS · Transistors · MOS · MEMS · Polymer-MEMS · Flexible PCB · PCB · Soft robotics · Smart textile · Intelligent textile · TFT · Organic TFT · Extended gate

5.1 Historical Perspective

Tactile sensing has been a component of robotics for roughly as long as artificial vision and auditory sense modalities. Tactile sensing began to develop in the 1970s—albeit at a slower pace, when compared with the development of other sense modalities. Early surveys on the state of tactile sensing show a wide diversity in the types of sensing device that were developed in the 1980s [1, 2]. Early works on tactile sensing focused on the creation of sensor devices using new transduction techniques and a large number of experimental devices and prototypes were built and reported in the literature. Particular attention was given to the development of tactile sensing arrays for the object recognition [3]. The creation of multifingered robotic hands, in late 1980s, increased the interest in tactile sensing for robotic manipulation and thus started appearing works utilizing tactile sensing in real-time control of manipulation [4–7]. The new applications demanded features such as mechanical flexibility and conformability and accordingly new designs and materials for tactile sensing received attention. While the development of tactile sensors for robotic fingertips and hands continued, the application areas such as motion planning in unstructured environment brought whole body sensing to the fore. As a result, many sensitive

R.S. Dahiya, M. Valle, *Robotic Tactile Sensing*,
DOI 10.1007/978-94-007-0579-1_5,

Table 5.1 The classification of various Tactile Sensing technologies

Transduction Medium/Method	Material	Sensor Structure
Resistive	Composites	Microelectromechanical systems (MEMS)
Capacitive	Carbon Nano Tubes (CNT)	Plastic MEMS
Optical	Conductive Polymers	POSFET
Magnetic	Force Sensing Resistors	Extended Gate Transistors
Ultrasonic	Pressure Sensitive Ink	Organic Field Effect Transistors (OFET)
Piezoelectric	Conductive Gels	Flexible Printed Circuit Boards (PCB)
Electrorheological	Conductive Fibers and Yarns	Mechanical Switches
Magnetorheological	Piezo-/pyroelectric Materials	
Electrochemical	Photoelastic Materials	

skin design projects were undertaken in the late 1980s and 1990s [8–10]. The application domain of robotics has been continuously increasing and the new generation of robots nowadays include social robots, rehabilitation and assistive robots, biorobots, medical robots and humanoids. Compared to the human controlled industrial robots, operating in "No-Humans" working zones, these new generation robots are characterized by close interaction with environment (including humans) and autonomous learning. In addition to the standard manipulation and exploration tasks, the new generation robots are also expected to interact safely. Tactile sensors distribution over the entire body is indispensable to build service robots that can co-exist with humans for support and enhancement of human life. The full-body tactile sensor could generate more tactile information than in the case where only joint force and moment are measured. As a result, nowadays there is an increased interest in developing large area or whole body tactile sensing structures that allow a robot to safely carry out a task while maintaining physical contact [11–13].

Analyzing the present state of research in the area tactile sensing, three strategies emerge for the development of tactile sensing units in robots [14]: (1) developing sensors based on various methods of transduction; (2) development of structures that generate a signal on touch; and (3) the use of new materials that intrinsically convert mechanical stimulus on touch into usable signals. This classification of tactile sensing technologies is given in Table 5.1 and explained in this chapter along with their merits and demerits. The working principle of various methods have been explained and selected implementations are presented. Quite often the tactile sensing schemes belong to one or more aforementioned strategies, which is also reflected by some of the implementation presented in this chapter. The overview presented here also takes into consideration the reviews on the state of research in tactile sensing reported in literature from time to time [2, 4, 7, 13, 15–22].

5.2 Tactile Sensing Based on Various Transduction Methods

The transduction methods described in this section are listed in Table 5.1. These methods can be divided in to two categories: Firstly, the methods with coupled mechanical and electrical transduction—for instance, the capacitive, resistive, and ferroelectric methods, where deformation of the sensor surface due to object contact causes a change in an electrical parameters of the sensor material. Second, the methods with non-coupled electrical and mechanical transduction. Principle among these are the optical, ultrasonic, and magnetic transduction methods. This section describes all these methods in detail.

5.2.1 Resistive Sensors

Resistive tactile sensors utilize the change in resistance of the sensing material for detection and measurement of contact forces. The degree to which resistance of any sensing material changes depends on: (a) the contact location (e.g. potentiometer type); (b) the contact force or contact pressure (e.g. piezoresistance, and elastoresistance). Accordingly, the resistive tactile sensors can be grouped in two categories.

Resistive sensors based on the first type, are either made of two-dimensional grid of sensing elements or composed of two flexible sheets coated with a resistive material (with finite resistivity, typically on the order of 100 Ω/sq.) placed on top of each other and separated by air, microspheres, insulating fabric etc., as shown in Fig. 5.1(a). Accordingly, former arrangement is termed as discrete resistive touch sensing and latter as analog resistive touch sensing. The scheme of analog resistive touch sensing, in typical 4-wire configuration, is shown in Fig. 5.1(a)–(f). During operation, a uniform, unidirectional voltage gradient is applied to the first sheet, as shown in Fig. 5.1(b). When the two sheets are pressed together the second sheet serves like the slider in a linear potentiometer and measures the voltage as distance along the first sheet, thus providing the X coordinate. When this contact coordinate has been acquired, the uniform voltage gradient is applied to the second sheet to ascertain the Y coordinate. The complete method of ascertaining contact location is given in Fig. 5.1(b)–(f). As voltage V_x or V_y is applied over the X or Y plane and the voltage V_{xout} or V_{yout} measured at any of the analog high impedance (Hi-Z) terminals is approximately given by:[1]

[1]The actual expressions of V_{xout} or V_{yout} are:

$$V_{xout} = \frac{R_{x2}R_L}{R_{x1}R_L + R_{x2}R_L + R_{x1}R_{x2}}V_x \qquad V_{yout} = \frac{R_{y2}R_L}{R_{y1}R_L + R_{y2}R_L + R_{y1}R_{y2}}V_y \tag{5.1}$$

where, R_L is the resistance seen from contact point toward the measurement terminal i.e. $R_{touch} + R_{y1}$ (or R_{y2}) + Hi-Z. When impedance at the measuring terminal is high, these expressions in (5.1) reduce to (5.2)–(5.3).

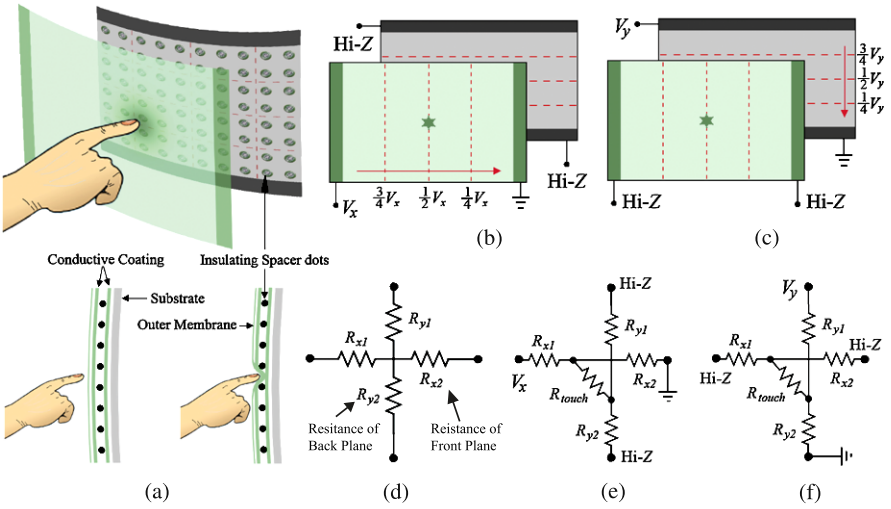

Fig. 5.1 (**a**) The scheme of analog resistive touch sensing; (**b**) X coordinate measurement: Voltage gradient applied across the front sheet and voltage measured at any of the Hi-*Z* terminals of back sheet; (**c**) Y coordinate measurement: Voltage gradient applied across the back sheet and voltage measured at any of the Hi-*Z* terminals of front sheet; (**d**) Circuit configuration under untouched condition; (**e**) Circuit configuration for measuring X coordinate; (**f**) Circuit configuration for measuring Y coordinate

$$V_{xout} = \frac{R_{x2}}{R_{x1} + R_{x2}} V_x \tag{5.2}$$

$$V_{yout} = \frac{R_{y2}}{R_{y1} + R_{y2}} V_y \tag{5.3}$$

proportional to the X or Y coordinate of contact point. Both the sampling of the two voltages and the subsequent calculations are very simple and the operation occurs instantaneously, registering the exact touch location as contact is made. In addition to the contact location, the touch pressure (or Z axis measurement) can also be measured by relating pressure to the resistance [23].

Analog resistive touch sensing technology typically results in high resolution (4096×4096 DPI or higher) and high response speed (10 msec or higher), thus providing fast and accurate touch control. However, the approach results in detection of only one contact location. While suitable for the touch screens of appliances such as personal digital assistants (PDAs), and as generic pointing devices for instruments, the analog resistive sensing technology has limited utility for robotic applications where simultaneous multiple contacts are often observed. With some design modifications the multiple contacts can be measured and hence analog resistive sensing technology can be adapted for robotic applications. Among others, the hybrid resistive tactile sensing [24] is one such technique that allows measurement of multiple contact points. Hybrid resistive sensing is a combination of the analog resistive and the array touch sensing technologies. It also involves two sheets of

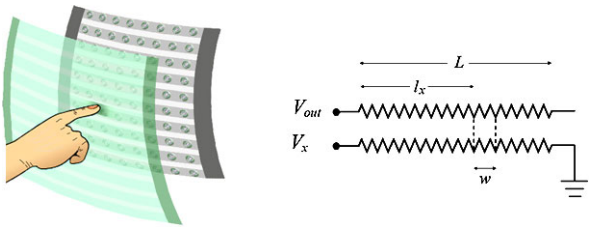

Fig. 5.2 The scheme and equivalent circuit diagram of hybrid analog resistive touch sensing

conductive materials, one on top of the other. However, one or both sheets are divided into multiple strips aligned along their lengths. One such scheme, with both sheets divided into multiple strips, is shown in Fig. 5.2. In this way, the configuration looks like one-dimensional arrays of stripped analog resistive sensors described earlier and the contacts can be sensed along different strips separately. The sensor measurement, along a strip, depends on both the location and the length of contact along each strip. Following a simple circuit analysis, the output of the sensor equivalent shown in Fig. 5.2 can be obtained as:

$$V_{out} = \frac{l_x + w/2}{L - w/2} V_{ref} \tag{5.4}$$

where, V_{ref} is the reference voltage applied across the sheet, w is the contact width, l_x is the contact distance from one of the ends as shown in Fig. 5.2, and L is the length of the strip. Because the sensor is discretized in one direction, each scanning of the sensor produces a set of at least n measurements from which the contact shape is to be reconstructed. In comparison with the n^2 operations needed with a conventional matrix sensor configuration, the number of measurements, and hence the scanning time, is much lower in case of hybrid resistive tactile sensing. The number of measurements in each scanning will, however, become $2n$ if two measurements are made for each contact point—as in analog resistive touch sensing described earlier. Similarly, the scheme discussed above requires a minimum of $n + 2$ connectors/wires (one for the V_{ref}, one for common ground, and n for the sensing the individual strips) against $2n$ (without MUX) needed with a conventional matrix sensor configuration.

Piezoresistive touch sensors are made of materials whose resistance changes with force/pressure. Touch sensing system using this mode of transduction have been used in anthropomorphic hands [25]. Piezoresistive tactile sensing is also popular among the MEMS based and silicon based tactile sensors [26–28]. Some examples of piezoresistive sensors are given in Fig. 5.3. These examples also include the sensors that are based on MEMS approach. The MEMS based tactile sensors are described later in the section on tactile sensing structures.

Recently, the piezoresistive tactile sensors have been realized using materials such as conductive rubber, conductive polymers, conductive gels, conductive fibers and yarns, force sensing resistors (FSR), and pressure sensitive ink etc. Sometimes, the changes in resistance of a conductive elastomer or foam is also termed as elastoresistance or elastoresistivity. However, for simplicity, the term piezoresistance is used in this book. Some of these materials are described later in this chapter.

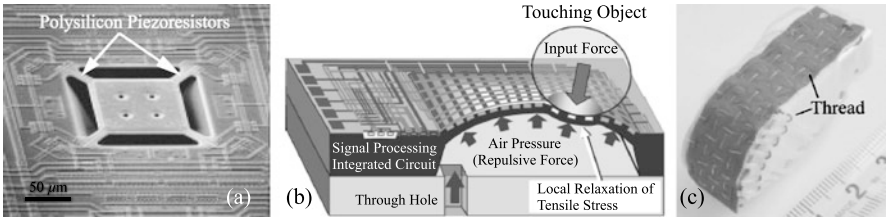

Fig. 5.3 (**a**) An example of piezoresistive based MEMS traction stress sensor consisting of a plate suspended with four bridge structures. (Characteristic dimensions: bridge $= 22 \times 12 \times 2.35$ μm, plate $= 100 \times 100 \times 2.85$ μm, pit depth ≈ 100 μm.) A polysilicon resistor is embedded in each bridge (with permission from [28], ©(2000) IEEE); (**b**) An example of piezoresistive based flexible MEMS sensors array (with permission from [30], ©(2006) IEEE); (**c**) Pressure conductive rubber based touch sensor with wires stitched on it (with permission from [31], ©(2004) IEEE)

The tactile sensors based on a conductive polymer film called FSRs are widely used in pointing and position sensing devices such as joysticks and are commercially manufactured by Interlink [29]. FSRs have rows on one flexible substrate and columns on another. They also feed the output voltage back to the other columns to eliminate a flow of current between the measured column and the others. It takes about 25 μs for the feedback loop to settle. Unlike other conductive polymer, patterned FSRs therefore do not have in-plane conduction between the rows, which reduces sensitivity. The FSR sensors are appealing, because of the low cost, good sensitivity, low noise and simple electronics and, in fact, can be found in many experimental tactile systems. One of their drawbacks is the relatively stiff backing. Although examples of advanced robotic hands equipped with FSRs exist [32, 33], these sensors generally require serial or manual assembly, provide highly non-linear response and suffer from hysteresis.

A number of touch sensors using pressure conductive rubber as transducer have also been reported [31, 34]. They take advantage of change in impedance due to the applied force/pressure. One such sensor by Shimojo et al. [31] is shown in Fig. 5.3. The horizontal and vertical wires (i.e. rows and column wires) are stitched into a layer of conductive rubber and the sensing elements of the array are formed at the intersections of the rows and columns. A total of 16×3 sensor elements are obtained in an area of 44 mm $\times$ 12 mm, with a pitch of 3 mm. The sensor elements show a repeatable but non-linear and hysteric response to applied pressure in the range of 0–200 kPa. The delay between input and output is reported to be 1 ms, which is expected to go up if the time taken by rubber to regain the original shape is also considered. Presence of hysteresis and non-linearity are some of their drawbacks.

In recent years, the stretchable tactile distribution sensors based on conductive sheets (made of one or more layers of conductive materials) have been developed [35–37]. The electrical impedance tomography EIT[2] technique is employed in these

[2]Electrical impedance tomography (EIT) is an imaging technique used to estimate the internal conductivity distribution of an electrically conductive body by using measurements made only at the boundary of the body. The technique is also used in non-invasive medical applications.

sensors to obtain the contact information. In this method, a conductive material with electrodes placed on its boundaries is used as the tactile sensor. The current is injected into the sheet via electrodes and impedance distribution is observed. On application of pressure, the impedance distribution changes resulting in to the change in current distribution, which can be quantified using EIT. The tactile sensing scheme can be used to detect contact events such as stroking, pinching and grabbing. Since most of the sensing area in an EIT based sensitive skin is made of an homogeneous thin material without any wiring, a large, flexible and stretchable skin suitable to cover small and large areas of variable three dimensionally contoured bodies can be realized. The requirement of continuous current injection (and hence loss of energy) is a major area of concern that can hinder effective utility of this approach, especially in the autonomous robots that rely on battery power.

Tactile sensors based on quantum tunneling composites QTC have also come up recently and commercially available from Peratech [38]. QTC's have the unique capability of transformation from a virtually perfect insulator to a metal like conductor when deformed by compressing, twisting or stretching of the material. These materials are described later in this chapter.

The resistive tactile sensing technology is economical and simple to construct and use. Further, the complexity does not increase with the size of the sensor surface and the sensor can be produced with inexpensive materials. Another issue with resistive touch sensing technology is the higher power consumption.

5.2.2 Capacitive Sensors

The capacitive measurement methods have been used for a long time in many applications to measure physical values like distance, pressure, liquid level, acceleration, humidity, and material composition etc. The newer applications, widely using capacitive touch technology, include human–machine interfaces applications such as laptop track pads, computer displays, mobile phones and other portable devices. The capacitive measurement methods are also widely used in many MEMS based touch sensing arrays such as those for high resolution tactile imaging of fingerprints. The techniques has also been employed in robotics to detect contacts over large areas of a robot's body.

At the heart of any capacitive sensing system is a set of conductors that interact with electric fields. Typically, the capacitive sensors are the plate capacitors (Fig. 5.4), consisting of two identical and parallel metal plates or electrodes of area A separated by a distance d with a flexible spacer (usually, silicone or air) of relative dielectric constant ε_r. The basic principle behind working of a capacitive sensor is detection of the change in capacitance when something or someone approaches or touches the sensor. The capacitance of a parallel-plate type capacitor (Fig. 5.4) is given as:

$$C = 4\pi\varepsilon_r\varepsilon_0\frac{A}{d} + C_f \tag{5.5}$$

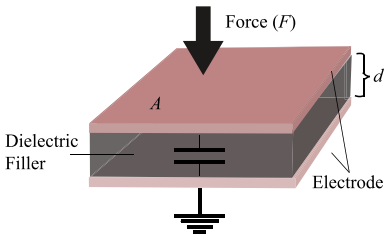

Fig. 5.4 A parallel plate capacitor consisting of tow parallel plates of area A, separated by a flexible insulator of relative dielectric constant ε_r. The thickness of the dielectric film is d

where, ε_0 is the (electric) permittivity of a vacuum, and C_f is the contribution from edges of the electrode (which tend to store more charge than the rest of the electrode). Typically, $A \gg d^2$ in all designs for tactile sensors, therefore, the C_f term is negligible. The distance between the electrodes is usually lower, as the inverse relation between capacitance and gap between electrodes is highly non-linear and the sensitivity drops significantly with larger gaps.

When a force is applied on the capacitive sensors, it changes the distance between the plates or the effective area—resulting in the changed capacitance. The normal force changes the distance between the plates while tangential force changes the effective area between the plates. The capacitive sensor are thus capable of detecting touch by sensing the applied normal or tangential forces; however, they are not efficient enough to distinguish these two types of forces. The change in capacitance is eventually converted into a change in voltage by using an appropriate circuit[3] and a measure of the applied force is obtained. The capacitive sensors therefore convert the physical input signal to the output signal in two steps: firstly, by transducing a physical quantity into a change of electric capacitance; then, by measuring and converting the capacitive signal into an electric output signal.

The capacitive touch sensing systems are of two types: the self- or absolute capacitance type, where the object (such as a finger) loads the sensor or increases the parasitic capacitance to ground; and the mutual capacitance type, where the object alters the mutual coupling between two electrodes.

The self capacitance is defined as the capacitive load, relative to circuit ground, that an electrode presents to the measurement system. A self capacitance type touch sensor, shown in Fig. 5.5(a), has one electrode that represents one plate of the capacitor. The corresponding second plate is represented by the environment of the sensor electrode and another conductive object, like a human finger, to form a parasitic capacitor $C_{Electrode}$. The sensor electrode is the only direct connection to the sensor controller. The capacitance of the sensor pad is measured periodically. When a conductive object, like a human finger approaches or touches the electrode, as shown in Fig. 5.5(b), the measured capacitance will increase by a value C_{Touch}

[3]The measurement circuits used to measure the capacitance change are based on methods like, relaxation oscillator, Charge time versus voltage, Voltage divider, Charge transfer, and Sigma–Delta modulation etc. The capacitance changes are measured using parameters like shift of resonance frequency, frequency modulation, amplitude modulation, charge time measurement, time delay measurement, and duty cycle etc.

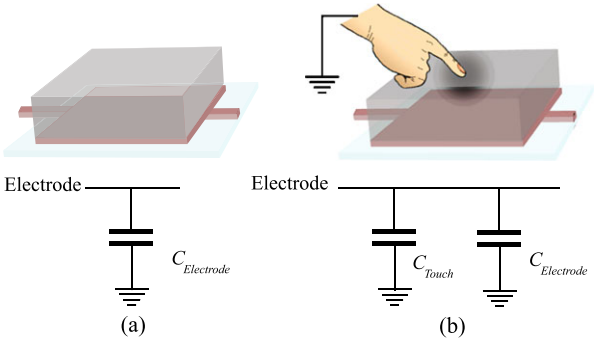

Fig. 5.5 (**a**) The self-capacitance type touch sensor with parasitic capacitance $C_{Electrode}$; (**b**) The additional capacitance C_{Touch} is generated when a conductive object touches the sensor

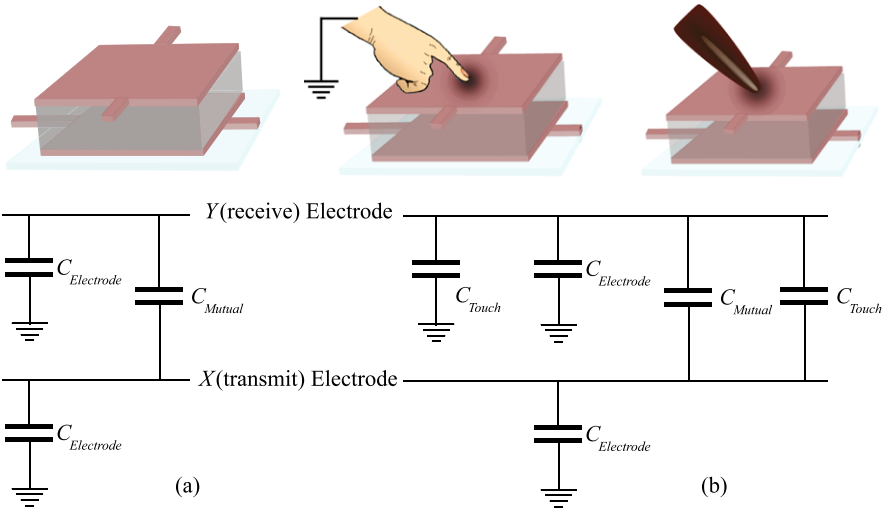

Fig. 5.6 (**a**) The mutual-capacitance type touch sensor. $C_{Electrode}$ is the parasitic capacitance of electrodes and C_{Mutual} is the mutual capacitance between electrodes; (**b**) The additional capacitance C_{Touch} is generated when any object touches the sensor

and the change is detected by the measurement circuit. The capacitance of touch is dependent on sensor design, sensor integration, touch controller design and the touch itself. These sensors tend to emit electric fields in all directions, and as such are quite non-directional. They are prone to false signals from parasitic capacitive coupling. Measuring self capacitance does not easily lend itself to supporting simultaneous multiple contacts, which requires correlation of multiple X and Y touched electrodes into multiple (X, Y) touch coordinates.

The mutual capacitance type touch sensors have two electrodes: an X (transmit) electrode, and a Y (receive) electrode, as shown in Fig. 5.6. The mutual capacitance is the capacitive coupling between the two electrodes. The arrangement is typically

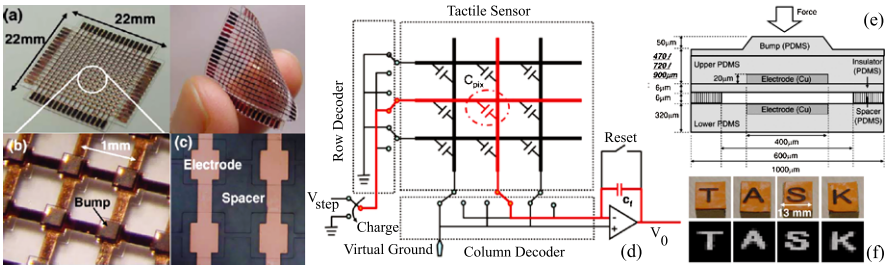

Fig. 5.7 (**a**) The capacitive tactile sensing module; (**b**) The magnified view of the sensing elements; (**c**) The bottom electrodes and the spacers; (**d**) The schematic of the readout circuit; (**e**) The cross-section view of one of the tactile sensors; (**f**) Flipped photographs of rubber stamps and their tactile images captured by the tactile sensing module (with permission from [39], ©(2006) IEEE)

used in array type tactile schemes, with the intersection of each row and each column making a capacitor. A 16×16 array, for example, would have 256 independent capacitors. A voltage is applied to the rows or columns. Bringing an object near the surface of the sensor changes the local electric field which reduces the mutual capacitance. The mutual capacitance from X and Y is measured by the sensor controller. The arrangement of electrodes may differ from the one shown Fig. 5.6. For instance, the two electrodes can also be in same plane as in interdigitated structures. Further, different electrode patterns can be used to create a capacitive sensor. The electrode pattern geometries are an important factor in the overall resolution and touch sensitivity of the sensor. The advantages of mutual capacitance based touch sensors include their ability to detect accurately the multiple contacts at the same time.

The mutual capacitive type touch sensors are more suitable (than the self capacitive type sensors) for robotics applications as the arrangement allows contact detection for human fingers (or conductive objects) and other objects. They can be made by using micromachined silicon technology as well as by the conventional non silicon technology. They can therefore be miniaturized, allowing construction of dense sensor arrays as in many MEMS capacitive sensors, or can be to made larger and suitable to cover various body parts of a robot. Examples of dense tactile sensing arrays include the tactile sensing array by Lee et al. [39], consisting of 16×16 capacitive cells or sensing elements. The key features of this capacitive tactile sensor array, shown in Fig. 5.7(a)–(c), include its mechanical flexibility (owing to its construction using multiple PDMS layers) and scalability. The capacitive tactile elements are formed at the intersection of the orthogonal row and column (or upper and lower) copper electrodes. For maximum sensitivity, air gap (as dielectric) is encapsulated between the electrodes at each intersection. The sensor size and electrode size are $600 \times 600\ \mu m^2$ and $400 \times 400\ \mu m^2$, respectively. The capacitance change at every individual point on the grid is measured to accurately determine the touch location by measuring the voltage in the other axis. The read out scheme employed for this purpose is given in Fig. 5.7(d). The capacitance C_{Mutual} of an element is read in 100 μsec (20 frames per second) by first selecting it with the help

of row and column decoders. The voltage V_{step} is applied to row electrode of this sensor to charge the capacitor. When V_{step} is switched to ground, the stored charge in the capacitor is transferred to the feedback capacitor C_f and changes the output voltage V_0 as:

$$\Delta V_0 = -\Delta V_{step} \frac{C_{Mutual}}{C_f} \tag{5.6}$$

The resolution of tactile sensor response is 1 mN and the full scale range is 40 mN (250 kPa). This capacitive tactile sensing systems is scalable, as multiple modules can be stitched with each other. Realized using MEMS approach, the sensor is composed of five PDMS layers (Fig. 5.7(e)), with the two copper electrodes embedded in the PDMS membrane. Using PDMS elastomer is as a structural material is useful in obtaining a mechanical flexible and compliant tactile sensing array. However, it is challenging to precisely control the thickness of various PDMS layers. For the same applied force, the variation of thickness of various layers results in variation among the responses of various sensing elements in the array.

The examples of capacitive touch sensors obtained using non-silicon technology include, the array of 16 capacitive sensors by Schmidt et al. [40]. The sensor couple to the objects being grasped via small brushes of fibers for dynamic sensing; thus providing two types of dynamical tactile information—speed and vibration—as analogous to the two types detected by human skin. This arrays furthermore is paired with two foil-based piezoresistive force sensors for static sensing. The sensor elements on the array are sensitive (with a threshold of about 5 mN) and robust enough not to be damaged during grasping. Commercially available touch sensors such as 'RoboTouch' and 'DigiTacts' from Pressure Profile Systems [41] are other examples of capacitive touch sensors obtained using non-silicon technology.

Recently, the capacitive (and also resistive) touch sensing technology has made its way to the human–machine interface applications such as mobile phones and other portable devices. The development of 'capacitance to digital converter' Integrated Circuit (IC) chips like 'AD7147 and the AD7143 from Analog Devices [42] has also contributed to wide usage of capacitive technology. These chips provide excitation to the capacitance sensor, sense the changes in capacitance caused by the user's proximity, and provide a digital output. The availability of these chips have made it easier to design paper-thin and reliable contemporary touch controls for the capacitive technology based sensitive touch sensors. Availability of these capacitance to digital converter chips has also been helpful to robotics. The capacitive robotic tactile sensing solutions, utilizing these chips have recently been reported by Maggialli et al. [43]. The tactile skin developed in European Commission funded project 'Roboskin', described later in this chapter, extensively employs these integrated circuits with capacitive tactile sensors to cover various lesser sensitive body parts of robots. Touch sensors based on capacitive mode of transduction are sensitive, easy to fabricate, and immune to temperature variations, but stray capacity and hysteresis are major drawbacks.

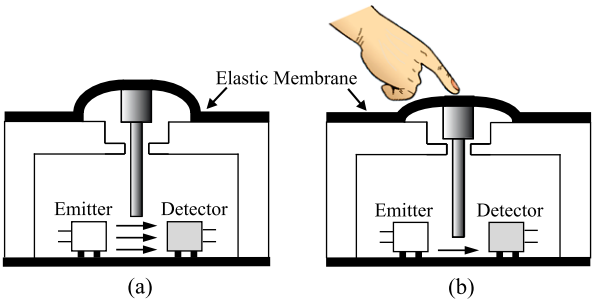

Fig. 5.8 (**a**) The optical transducer before applying the force or before contact; (**b**) The opaque pin moves downward after contact and blocks the block path of light between *emitter* and *detector*, thereby reducing the intensity of light received by *detector*

5.2.3 Optical Sensors

The optical mode of transduction is another alternative for the tactile sensing in robotics. In simple terms, the optical sensing involves "injecting" light into a medium (generally, soft and deformable) and measuring the change in the amount or the pattern of light when force is applied. Depending on how the amount or pattern of light is detected, the tactile sensors based on optical mode of transduction can be grouped into two categories [44]:

1. The *extrinsic* optical sensors, where the physical stimulus interacts with the light external to the primary light path.
2. The *intrinsic* optical sensors, where the optical phase, intensity, or polarization of transmitted light are modulated without interrupting the optical path.

Sometimes, optical fibers are directly used as the transducers in the design of tactile sensors. Therefore, this could also be considered as the third category of optical sensors. The working of optical tactile sensors, along with selected examples are described below.

In case of extrinsic optical sensors, the transducer's surface, generally made of compliant material, has on its underside a grid of elongated pins, as shown in Fig. 5.8. When force is applied to the compliant surface, the pins on the underside move downward and block the light path or modulate the light transmission between emitter and detector. As evident from the names, the function of emitter (a light-emitting diode (LED)) is to emit the light and that of detector (a photodetector) is to detect the same. The amount of downward movement and the degree to which the light is blocked or allowed to pass, gives a measure of the applied force. Correspondingly, the more the applied force, less is the amount of light received by the detector. The major problems with this type of arrangement, especially when the compliant surface is made of rubber, include: creep, hysteresis, and temperature variations. Furthermore, calibration is needed for each emitter–detector pair. Unlike resistive or capacitive sensors, the construction of this type of sensor is quite labor intensive.

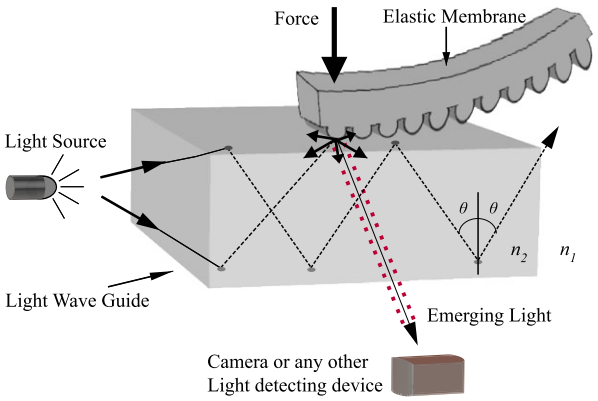

Fig. 5.9 The optical tactile transducer based on the principle of frustrated total internal reflection

The intrinsic optical tactile sensors normally utilize the change in intensity of transmitted light for measuring the tactile parameters such as contact force. Among various possible configurations, the one based on frustrated total internal reflection has been widely reported for the optical based tactile sensing. These tactile sensors use the properties of optical reflection between media of different refractive index, as shown in Fig. 5.9. The transducer structure is composed of a clear plate acting as light guide, a light source, a light detector and a compliant membrane stretched above, but, not in close contact with the plate. The lower surface of the plate acts as the imaging area. Light is directed along an edge of the plate and it goes through total internal reflection (when no force is applied) or diffuse reflection (when force is applied). The total internal reflection occurs when light is propagating in the denser of two media (i.e. refractive index, $n_2 > n_1$) and strikes the interface at an angle larger than a particular critical angle with respect to the normal to the interface (i.e. $n_2 \sin\theta \leq n_1$, where θ is the angle of incidence at the interface of two media). The light coming out of plate due to diffuse reflection can be recorded either by an array of photodiodes, solid state optical sensors, CCD or CMOS cameras placed in the imaging area or transported away from the sensor by optical fibers. The intensity of the light (bright or dark patches on image) is proportional to the magnitude of the pressure between object and plate. A weak point of these tactile sensors is the large consumption of current by various components.

With suitable design, this kind of sensor can also be made sensitive to shear forces. The optical waveguide based three axial tactile sensor by Okha et al. [45] is one such example. The sensing arrangement, shown in Fig. 5.10, designed in a hemispherical dome shape, mimicking the structure of human fingertips, consists of an array of 41 pieces of sensing elements made from silicon rubber, a light source, an optical fiber-scope, and a CCD camera. The silicone rubber element comprises of one columnar feeler and eight conical feelers. When sensor comes in contact with an object, the feelers collapse at the point of contact. At the points where the conical feelers collapse, light is diffusely reflected out of the reverse surface of the optical waveguide. The collapsed feelers are observed as bright spots in the image data

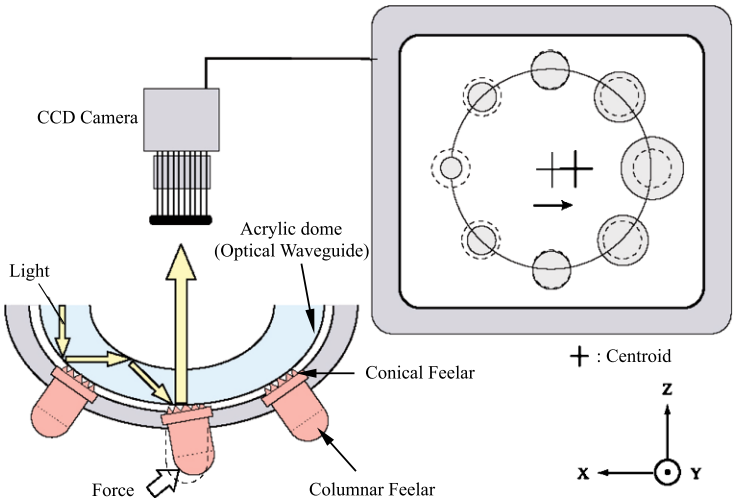

Fig. 5.10 Three-axis optical tactile sensor (with permission from [48]) capable of detecting forces in both normal and shear direction

acquired by the optical fiber-scope, connected to the CCD camera, and transmitted to the computer. In measurement process, the normal force of the F_x, F_y and F_z values are calculated using integrated gray-scale value, while shearing force is based on horizontal center point displacement. The sensor is capable of measuring normal and shear forces in the range 0–2 N, with a resolution of 0.001 N.

The intrinsic optical tactile sensing has also been used to develop the tactile sensing structures that can cover large body parts of a robot. Examples of such structures include the 32 element lightweight, conformable and scalable large area skin by Ohmura et al. [46]. The sensing element consists of photo-reflectors ($3.2 \times 1.1 \times 1.7$ mm) under the urethane foam (thickness 5 mm) and the light scattered by urethane foam upon deformation gives the measure of mechano-electrical transduction. The foam thickness controls the dynamic range and sensitivity of the sensors. This work is also explained later in the section on tactile sensing structures. The KINOTEX tactile sensors that use similar method, are also commercially available [47].

The fiber Bragg grating FBG based sensors also belong to the extrinsic optical sensors category. The basic principle of an FBG based sensor system lies in the monitoring of the wavelength shift of the returned Bragg-signal. The wavelength shift is a function of the parameter to be measured (e.g. strain, temperature and force). The 3×3 tactile sensor by Heo et al. [49] is an example of the FBG based optical tactile sensors. The sensor capable of measuring normal forces as low as 0.001 N with the spatial resolution of 5 mm.

Highly sensitive electrooptical tactile sensors based on CdS nanoparticles (capable of emitting visible light or the electroluminescence light on application of load) have been reported recently by Maheshwari and Saraf [50]. This tactile sensing is

described the next section, where many other new materials for tactile sensing are also described.

Many times fibers have also been used as transducers in the design of tactile sensor. As an example, the light coupling between adjacent fibers can be used to detect the contact events. Usually, the light propagates along an optical fiber with very little loss. However, the light can leave and enter the fiber from a point if its surface at that point is roughened. Therefore, light coupling can take place between two optical fibers passing close to each other, and both having a roughened surfaces. Measuring the increase in light attenuating due to microbending (which otherwise is considered as a disadvantage of the optical sensors) is another way of using the optical fiber as transducers. This effect has been put to use in microbend touch sensors by Winger and Lee [51]. The experimental 2×2 robot sensor is capable of detecting a 5 gm variation in the applied load within its linear region, which ranges between 125 gm and 225 gm per sensor element. The plastic optical fibers have also been used for the tactile sensor working on the principle of microbending [52]. With plastic optical fibers the limitations like rigidity and fragility can be overcome.

Some potential benefits of optical tactile sensors include, immunity to external electromagnetic interference, flexible, intrinsic safety, high resolution, low cost, and design simplicity. Some of the optical sensors suffer from the loss of light, for example by micro bending and chirping, causing the distortion in the signal. Owing to the paraphernalia needed to emit (source) and receive (detector) the light, at times they are bulky and it is difficult to reduce their dimensions. With the advent of smaller surface mounted silicon components it is possible to mount the small light emitter and detector pair inside the sensing element itself—raising hopes for small size optical tactile sensing systems.

5.2.4 Magnetism Based Sensors

The touch or tactile sensors based on magnetic transduction are developed using two approaches. Firstly, the sensors measuring the applied force led change in the magnetic flux using either the Hall effect or magnetoresistance.[4] Second, the sensors measuring the change in the magnetic coupling or change in the inductance of a coil as a result of applied force or pressure. A few tactile sensors using these approaches have been reported in literature [53–55].

[4]The charge carriers flowing through a conductive material, in presence of a magnetic field, experience a force orthogonal to their flow directions and the magnetic field direction. As a result the charge carriers are deflected, leading to the appearance of Hall potential in direction of the deflection. This is termed as Hall Effect. Due to this deflection, the charge carriers take a longer path to travel the length of the conductive material, meaning that the deflected particles have a lower mobility and hence an increased electrical resistance. This effect is known as magnetoresistance. Both the Hall effect and magnetoresistance can be used to measure magnetic field intensity.

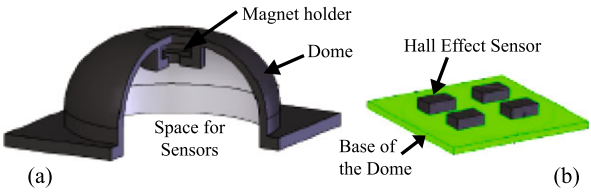

Fig. 5.11 Compliant magnetic tactile sensor (with permission, from [55]). (**a**) Silicone rubber dome as compliant cover. (**b**) Circuit board using hall effect sensors to detect deformation

If a very small permanent magnet is held above the Hall effect type detection device by a compliant medium, the change in flux caused by the magnet's movement due to an applied force can be detected and measured. The field intensity follows an inverse relationship, leading to a nonlinear response, which can be easily linearized by processing. In case of the Hall effect type detection devices, the change in magnetic flux is reflected into the change in Hall voltage, which can be easily measured. In a similar way, the magnetoresistance type detection devices are also used. It may be noted that a Hall effect sensor is only sensitive to magnetic fields in one direction while the magnetoresistive effect can be used to detect magnetic field having any orientation within a plane normal to the current flow. An example of Hall effect type tactile sensing arrangement is given in Fig. 5.11 [55]. This tactile sensing arrangement by Eduardo et al. has a small magnet embedded in the top of the dome. The base of the dome is glued to a printed circuit board (PCB), which also contains four Hall effect sensors. The difference in the signals from these four sensors is used to detect roughly the lateral displacement and the average of signals is used to obtain the vertical displacement. Four domes, similar to the one shown in Fig. 5.11(a), have been used at each phalange of robot's finger. The sensitivity of the sensor can be controlled by changing the shape of the domes. The optical version of this sensing arrangement has also been presented by Eduardo et al. [56]. All these sensing arrangements can detect normal, lateral and shear forces. Further, they can deal with the saturation when applied forces are out of range. The arrays of sensors by Eduardo et al. [55, 56] have also been tested in robots like Obrero and GoBot while doing actual tasks.

In the case of sensors measuring the change in the magnetic coupling or change in the inductance of a coil as a result of the applied force or pressure, the core of the inductor is generally made of magnetoelastic materials. The magnetoelastic materials deform under pressure and cause the magnetic coupling between transformer windings, or a coil's inductance to change. These materials change their magnetic permeability when they are deformed. A sensor array of 16×16 magnetoelastic sensor elements with 2.5 mm spacing has been reported by Luo et al. [57].

The tactile sensors based on magnetic principle have a number of advantages that include high sensitivity and dynamic range, no measurable mechanical hysteresis, a linear response, and physical robustness. They are capable of measuring three dimensional force vectors. Major drawback of magnetic based tactile sensor is that they cannot be used in magnetic medium.

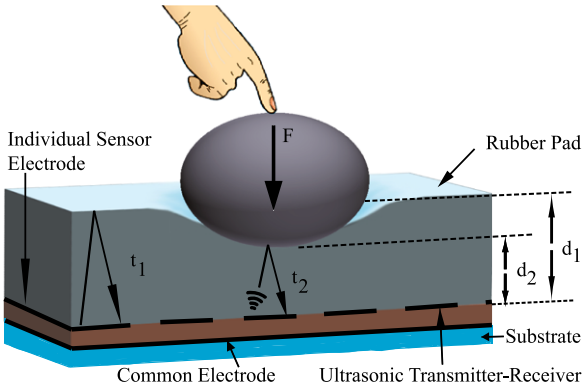

Fig. 5.12 Working of an ultrasonic tactile sensor

5.2.5 Ultrasonics Based Sensors

The ultrasonic transduction for tactile sensing is one of the methods where mechanical transduction is decoupled from electrical transduction. A typical ultrasonic sensing arrangement, shown in Fig. 5.12, involves a thin rubber covering that is deformed when an object presses into it. The amount of this deformation depends upon the magnitude of the force applied to the object and the stiffness of the rubber. Underneath this rubber covering are ultrasonic transmitters and receivers. The ultrasonic transmitters launch a small ultrasonic pulse of a few megahertz into the rubber pad. This pulse then propagates through the pad and is reflected from the exposed surface of the rubber. The reflected or echo pulse is received by the receiver, which is usually the same element that launched it. The round-trip travel or transit time is proportional to the thickness of the rubber pad overlying a particular tactile element. Therefore, by measuring the change in the round-trip travel or transit time (i.e. $t_1 - t_2$) of the pulse, it is possible to measure parameters like change in the thickness of the rubber pad (i.e. $d_1 - d_2$) and hence the applied force. The operation of the sensor can be expressed as:

$$d_1 - d_2 = \frac{1}{2}(t_1 - t_2) \tag{5.7}$$

$$F = k(d_1 - d_2) = \frac{1}{2}k(t_1 - t_2) \tag{5.8}$$

where, F is the compressing force, c is the speed of propagation of the ultrasonic wave in the rubber covering, and k is the rubber stiffness. Typically, the ultrasonic pulse transit times through the pad and back are on the order of few microseconds and changes in pad thickness of a few microns can therefore be detected. The strength of the echo pulse depends upon the acoustic properties of the rubber pad and the material contacting the pad.

The microphones based on ultrasonics have been used to detect surface noise occurring at the onset of motion and during slip. A 2×2 tactile array of polyvinylidene fluoride (PVDF), by Ando and Shinoda [58], senses contact events from their ultrasonic emission at the contact point. Here, PVDF polymer is used as receiver

to localize the contact point on a silicone rubber-sensing dome. The sensor is reportedly very effective in detecting slip and surface roughness during movement. The piezoelectric materials such as PVDF polymer and PZT are typically used as transmitters and receivers in the ultrasonic sensing applications.

The six-axis deformation sensing scheme by Ando et al. [59] is another example. The deformation sensing scheme is based on precise encoding and decoding of deformation components into ultrasound wavefronts. The arrangement consists of a 2×2 ultrasonic transmitter matrix and a 2×2 ultrasonic receiver matrix, placed face to face at a distance of a few tens of wavelengths. The prototype tactile sensor is embedded in a flexible hemispherical fingertip-like body. All of the transmitter elements are driven sinusoidally and simultaneously, but they are switched into the same, reversed, or quadrature phases to generate a particular shape of wavefront on the receiver matrix. The sensing scheme is able to detect three translational components and three rotational components of displacement around a transmitter position nearly simultaneously.

The resonant frequency of the piezoelectric materials changes when they come in contact with the objects having different acoustic impedances [60, 61]. The change in resonance frequency of the sensor, in accordance with the contact object's acoustic impedance, is also sometimes used to detect contact parameters. The change in resonance frequency has been used for detecting hardness and/or softness of objects [62] and to detect force/pressure [63]. Simple and elastic tactile sensors utilizing acoustic resonance frequency to detect contact parameters like principal stress, friction, and slip are also described in [64, 65]. The ultrasonic-based tactile sensors have fast dynamic response and good force resolution. However, many such sensors use materials like lead zirconate titanate (PZT), which are difficult to process in miniaturized circuits.

5.2.6 Piezoelectric Sensors

The piezoelectric transducers generating charge/voltage proportional to the applied force/pressure. They are also able to generate force due to applied electrical input. They can therefore be used both as sensors and actuators—the property that makes them 'Smart Materials'. The mechanical and electrical transduction are coupled in case of piezoelectric sensors. A simplified explanation of the piezoelectric phenomenon and the main concepts and working of piezoelectric sensors and transducers are given in Appendix A of this book.

A typical piezoelectric tactile sensor element has the same construction as the capacitance-based sensors (Fig. 5.4), where the dielectric material is piezoelectric with thickness t and area A. The piezoelectric material deforms by Δt on touching with contact force F to generate charges $+Q$ and $-Q$ at the two electrodes. As the element is also a capacitor, the induced charge leads to a potential V across the tactile element, as given by:

$$V = \frac{Q}{C} \approx \frac{dF}{C} = \frac{dt}{4\pi\varepsilon\varepsilon_r A} F \tag{5.9}$$

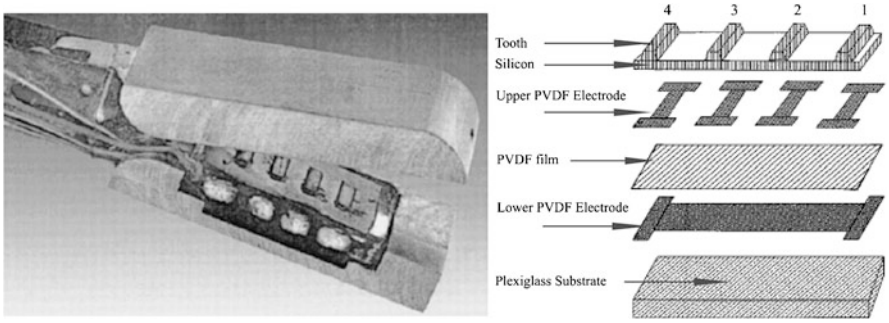

Fig. 5.13 An endoscopic grasper prototype integrated with the piezoelectric tactile sensor. The photograph (*left*) of the endoscopic grasper prototype and (*right*) the expanded view of the piezoelectric polymer PVDF based tactile sensor unit (with permission, from [66], ©(2000) IEEE)

where d is the piezoelectric constant of the material and C is the static capacitance. As given in Appendix A, d is a tensor with values depending on the orientation of the crystal in the film. For a simple uniaxial case (most often used) the tensor notation of d would be d_{33}. Similar to the capacitance-based device, the sensitivity of response to the applied contact force F is proportional to the signal V. However, in contrast to the capacitance device, the value of t should be large and that of ε_r should be low. In other words, to achieve high sensitivity, the d/ε_r ratio of the piezoelectric material must be as large as possible.

The piezoelectric sensors are highly sensitive with high voltage outputs even to small dynamic contact deformations. If a load is maintained, then the sensor output decays to zero. Therefore, these sensors are most suited for sensing dynamic forces. The sensing elements do not require power supply for its operation, and hence the sensor using piezoelectric transduction are reliable and efficient in terms of power consumption. Depending on the design of the sensor, different modes (longitudinal, transversal and shear) can be used to load the piezoelectric element. The tactile sensors based on piezoelectric transduction exhibit high sensitivity, a large dynamic range, a wide bandwidth with good linearity, and a high signal-to-noise ratio (SNR). The piezoelectric materials often used in tactile sensing schemes are described later in the section on tactile sensing materials.

A large number of tactile sensors, using either silicon micromachining technique or simply the polymer foils, have been reported in literature. A tactile sensor developed using PVDF piezoelectric polymer film and micromachining techniques is given in Fig. 5.13. This tactile sensor unit, by Dargahi et al. [66], is integrated with an endoscopic grasper suitable for minimally invasive surgery. The micromachined silicon part is patterned like a rigid tooth-like structure to transfer force to the PVDF film. As may be noted from Fig. 5.13, the sensor structure consist of three layers: the top layer, made of micromachined silicon to have a rigid tooth-like structure; the bottom layer, a flat plexiglass substrate; and, a 25 μm thick PVDF film sandwiched between the plexiglass and silicon. The top side of PVDF film consists of four strips of aluminum electrodes and the bottom side has a single common electrode. Four

output signals are therefore derived from the sensing device. When force is applied to any point on the surface of the silicon part, the stress in the PVDF results in a polarization charge at each surface. The difference between the response signals at four electrodes is used to indicate the localized position of the applied force.

A stress-component-selective tactile sensing array, based on piezoelectric polymers is presented in [67]. This multi-component touch sensing array consists of an assembly of seven elemental sub-arrays—each consisting of six miniaturized sensors, supported by a polyimide sheet and sandwiched between two elastic layers. Dario and Buttazzo [68] have developed a anthropomorphic robotic finger that uses piezoelectric polymer (PVDF) film as tactile sensor. This sensor contains two force-sensing layers and has the additional capability of sensing thermal properties. PVDF film sensors are also used in another implementation of robotic fingertip by Hosoda et al. [69]. In this arrangement, the PVDF films and strain gauges sensors are randomly embedded into a silicone layer.

Some other piezoelectric transduction based tactile sensors, including novel POSFET tactile sensing devices and the high resolution tactile sensing arrays, are discussed in Part II of this book.

In general, the piezoelectric transducers also exhibit pyroelectric properties, i.e. they generate charge/voltage when contact or ambient temperature changes. This is useful property as same sensor can be used to measure multiple contact parameters such as force and temperature. However, it is difficult to decouple or separate the responses when both piezoelectric and pyroelectric effects occur simultaneously. In such cases, the contribution from one of the effects could become significant source of noise in the overall response. For instance, if contact force is the parameter of interest, then ambient temperature variation may introduce noise in the overall response. Thus, protection from thermal variations may be necessary if force or pressure variations are important. Such errors can also be mathematically compensated, as explained later in Chap. 8, by recording the temperature variations with a temperature sensors and finding out corresponding pyroelectric response from pre-recorded database. The latter can then be subtracted from overall response to obtain the response due to force or pressure only.

5.2.7 Electrorheological Sensors

Some gels or electrorheological (ER) fluids have the ability to transform from a liquid to a plastic state, in milliseconds, on application of a strong electric field across them. This is known as the electrorheologic effect. The fluid viscosity of the ER fluid is proportional to the applied field strength. The ER fluids are a suspension of a dielectric solid or polymeric particles (the dispersed phase) in an insulating base oil (the continuous phase), which under normal conditions behaves as a Newtonian fluid. Examples of ER fluids include, silicone oil with $Na_{12}Al_{12}Si_{12}O_{48}$, and a nematic liquid crystalline (LC) E7 mixed with lithium polymethacrylate (LiPMA) [70]. A widely accepted description of the electrorheologic effect states that the dielectric solid particles in the fluid become polarized and form microstructures

(chains or clusters) under the presence of an electric field. Whereas a majority of applications use the ER fluids in shear mode, they are subjected to both shear and squeeze in case of tactile arrays.

A tactile actuator and a matching sensor, based on the aforementioned principle, is reported by Voyles et al. [71]. The actuator–sensor pair has male–female symmetry for the purpose of remote monitoring of touch sensing. The fingertip-shaped sensor detects contact events on its external surface using a gel layer as a dielectric in capacitive sensing, while the similarly shaped actuator recreates the remotely sensed tactile events on its internal surface by changing the solidity of areas of the gel in contact with the human operator. The ER fluid based robotic fingers have also been reported in literature [72].

The ER fluids are attractive because they are controlled electrically, which is convenient as there are no moving parts. They require little power (although voltages can be very high) and they can be made very compact. In fact, the smaller the dimensions, the higher the field strengths and the stronger the ER effect. These characteristics make ER fluids attractive for the haptic interfaces.

5.2.8 Magnetorheological Sensors

Similar to the ER effect, discussed above, there exists magnetorheological (MR) effect whereby the MR fluids exhibit rapid, reversible and significant changes in their rheological (mechanical) properties while subjected to an external magnetic field [70]. The MR fluids are suspensions of micron sized ferromagnetic particles dispersed in different proportions of a variety of nonferromagnetic fluids. As with ER fluids, the MR fluids are also in liquid state without external stimuli. While MR fluids are subject to a magnetic field, they behave as solid gels, typically becoming similar in consistency with dried-up toothpaste. In recent years, MR fluid based haptic displays and haptic interfaces have been investigated by some researchers. Carlson and Koester have developed a prototype of portable hand and wrist rehabilitation device based on MR fluid [73]. MR fluid have also been used to construct tactile and haptic displays to replicate perceived biological tissue compliance [74, 75]. The challenges of producing strong magnetic fields over large surface areas, however, limits the application of MR fluid sensors.

From above discussion it may be noticed that tactile sensors based on nearly all possible modes of transduction exist. Some of the least explored transduction methods not explained above include, electrochemical and acoustics methods. The advantages and disadvantages of some of the frequently used tactile sensing methods are summarized in Table 5.2. Some of these methods combine mechanical and electrical transduction (e.g. capacitive, resistive, and ferroelectric) and some other do not have such coupling (e.g. optical, ultrasonic, and magnetic). The main problem with coupled mechanical–electrical transduction schemes is the difficulty in optimizing one form of transduction without compromising the other. This is simply because there is no material with just the right combination of mechanical and electrical attributes. By separating the mechanical and electrical transduction in the sensor, both

Table 5.2 Merits and demerits of various tactile sensors types and implementations

Sensor Type	Merits	Demerits
Resistive	1. High Sensitivity	1. High Power Consumption
	2. Low Cost	2. Generally detect single contact point
		3. Lack of contact force measurement
Piezoresistive	1. High sensitivity	1. Stiff and Frail
	2. Low Cost	2. Non-linear response
	3. Low noise	3. Hysteresis
	4. Simple electronics	4. Temperature sensitive*
		5. Signal drift
Capacitive	1. Sensitive	1. Cross-talk
	2. Low Cost	2. Hysteresis
	3. Availability of commercial A/D chips	3. Complex electronic
Optical	1. Sensitive	1. Bulky
	2. Immune to electromagnetic interference	2. Loss of light by micro bending
	3. Physically flexible	3. Chirping
	4. Fast response	4. Power consumption
	5. No interconnections	5. Complex computations
Ultrasonic	1. Fast dynamic response	1. Limited utility at low frequency
	2. Good force resolution	2. Complex electronics
		3. Temperature sensitive
Magnetic	1. High sensitivity	1. Restricted to non-magnetic medium
	2. Good dynamic range	2. Complex computations
	3. No mechanical hysteresis	3. Somewhat bulky
	4. Robust	4. High Power consumption
Piezoelectric	1. High Sensitivity	1. Temperature sensitive
	2. Dynamic Response	2. Lacks robust electrical connections
	3. High bandwidth	3. Unsuitable for static contact events
Conductive rubbers/composites	1. Mechanically flexible	1. Hysteresis
	2. Easy fabrication	2. Non-linear response
	3. Low cost	3. Slow time response

forms of transduction can be optimized without compromising the other. Consider for instance, the elastic material typically used in the sensor covering can be chosen for the most appropriate combination of stiffness, resistance to abrasion, tearing, oxidation, chemicals and other environmental factors. Since the rubber covering simply overlies the sensor, it can be replaced when it is worn or damaged or when different rubber characteristics are required; such as less stiffness to provide higher force sensitivity.

5.3 Materials for Tactile Sensing

In the past, most devices have relied on fairly rigid, solid materials for their construction. Perhaps this was the natural choice to start as rigid systems are simpler and there are fewer variables to control or design. Nowadays, however, there is a demand for flexible large-area sensors that can be embedded, for example, into the flexible skin material of robotic fingers and used for sensing multiple locations. Taking cues from human tactile studies and the physical nature of the tissues and skin, it seems that softer materials may have much to offer. Elastic overlays and compliant contact surfaces are often advocated for their frictional and other properties, even if their low pass filtering behavior can be a disadvantage. Softer materials such as rubber, fluids and powders are therefore being examined. Some commercial touch sensors like those from Tekscan [76] using pressure sensitive ink or rubber are already available. Conductive gels have been considered for their remarkable softness showing a 20% change in impedance for pressure 0–400 kgf/cm^2 [77]. A range of materials with different consistencies have been examined in [78] for impact and strain energy dissipation conformability to surfaces and hysteresis effects. It is found that soft surfaces have more desirable characteristics for contact surfaces than hard materials. Among soft materials, gels are better than plastic, rubber, sponge, or paste, with powders being the second best. A range of materials used in various tactile sensing schemes are discussed in this section.

5.3.1 Piezoelectric Materials

Piezoelectric materials are insulators that generate charge when they are mechanically deformed or strained. As explained in Appendix A, the charge generation can occur in two ways: Firstly, due to specific crystal structure of the material—the deformation causes the cations and anions to move asymmetrically, thus leading to a high polarization; and, second by aligning the permanent dipole moment of the molecules forming the crystal. The piezoelectric effect arising from the crystal structure usually occurs in inorganic materials, such as $BaTiO_3$, the lead zirconate titanate class of ceramics ($Pb(Zr_xTi_{1-x})O_3$, PZT), ZnO, and CdS. The molecular effect is observed for macromolecules that have intrinsic permanent dipole moments, such as PVDF, and nylon [79].

A wide variety of materials, including PZT, ZnO, and $PVDF$ have been used to make tactile devices. As the material is not perfectly oriented, they are normally "poled[5]" in the direction orthogonal to the film plane to achieve maximum polarization. In this way the value of piezoelectric constant (d) is increased to the maximum that is practically feasible. The PZT and $PVDF$ are the materials of choice for

[5]Poling is the method of aligning or orienting the dipoles in a particular direction. Generally, poling is done by applying a strong electric field (sometimes in combination with mechanical processes such as stretching), whose direction also sets the direction of polarization.

tactile sensing because of the requirements for high sensitivity, ease of fabrication, and mechanical properties. In particular, PZT has a higher piezoelectric constant ($d_{33} = 117$ pC/N) than single-crystalline materials such as quartz ($d_{11} = 2.3$ pC/N) and zinc oxide ($d_{33} = 12$ pC/N), and additives can be used to alter its electrical and mechanical properties. PVDF has a lower piezoelectric constant ($d_{33} = 30$ pC/N), but its much lower ε_r value (100-fold lower than PZT) makes it an ideal material to make tactile devices [80]. Furthermore, the polymers such as PVDF have some excellent features, such as, mechanical flexibility, workability and chemical stability [81]. The low cost and ease of processing the polymer (compared to ceramics) has also led to its wide use as a piezoelectric material. A marked phenomenological analogy exists among epidermis sample of human skin and PVDF [82]. The PVDF or its copolymers have been used in a large number of tactile sensing schemes, including one based on piezoelectric effect and also the ultrasonics [66, 83–86].

5.3.2 Conductive Polymer Composites

The conductive polymer composites (CPC) are becoming popular and offering attractive alternatives for developing new generation of mechanically flexible tactile sensing devices that can be wrapped around curved surfaces and spanned over large areas (tens of cm^2). The CPCs are obtained by adding micro/nano sized conductive filler particles or structures to an insulating polymer matrix. Incorporation of conductive fillers into a host polymer/elastomer matrix constitutes an excellent approach for the development of special materials, which combine electronic conductivity with elasticity and other important mechanical properties imparted by the insulating rubber (polymer/elastomer) matrix. Investigators have used conductive filler materials such as carbon based fillers (e.g. carbon black, graphite powder, carbon fibers) and metal particles or metal flakes (e.g. Ni, Cu, Ag, Al and Fe). On compression the polymer matrix deforms and the filler particles are brought closer, thereby causing an increase in conductivity. Therefore, the sensor based on these materials are essentially piezoresistive in nature. The transition of the composite from insulator to conduction, commonly explained using statistical models and percolation theory [87–89], takes place when the volume fraction (V_c) of the conductive filler particles is above a certain value, which is called percolation threshold.[6] The conductivity rises at the percolation threshold as the conductive particles begin to aggregate to produce chains of particles in intimate contact, providing conductive paths spanning the sample. The conductivity increases rapidly as more percolation paths form until saturation is approached, when the conductivity rises slowly to its

[6]The percolation theory model fails below the percolation threshold, where it predicts that the composite is an insulator. Effective medium theories have been developed that provide a good description of the evolution of the conductivity across the full range of filler concentrations. Discussion on such theories is beyond the scope of this book and reader may refer to relevant literature [87].

maximum value or resistance (or piezoresistance) falls to minimum value. Theoretically, the percolation threshold for uniformly dispersed (random distributed) particles is about 16% by volume [90]. In practice, however, the value may vary between 1–30% as it depends on the shape and size of the filler particles, which affect their spatial distribution [19]. If relationship between compressive strain, conductivity, and the mechanical properties of the composite film are known, the local strain (and stress) can be obtained by measuring the local conductivity through the film.

Several conductive polymer composites have been explored for tactile sensing. Depending on the type of filler particles, they can be categorized as composites with: (a) metal nanoparticle fillers; (b) conductive polymer nanoparticle fillers; (c) carbon microcoil fillers; (d) graphite nanosheet fillers; (e) carbon black nanoparticle fillers; and (f) carbon nanotube (CNT) fillers. These conductive polymer composites are explained below, with suitable examples.

5.3.2.1 Conductive Polymer Composites with Metal Nanoparticle Fillers

The conductive polymer composites with metal nanoparticle fillers include QTC (Quantum Tunneling Composites) by Peratech [38], which consists of nickel particle (with sharp projections) in silicone matrix. Typically silicone rubber matrix is used in various composites because it has excellent elastic, thermal, and mechanical properties and a very good environmental stability. The QTC sheets are mechanically flexible and the flexibility depends on the grade of elastomer used as matrix, the filler loading and the sheet thickness. Thin sheets with low filler loading are the most flexible. The principal conduction mechanism depends on the tunneling between filler particles, which is evident from the exponential dependence of sample response on deformation. In QTCs the metal particles never come into contact. Rather they get so close that quantum tunneling (of electrons) takes place between the metal particles. The transition from insulator to conductor follows a smooth and repeatable curve, with the resistance dropping exponentially. Under modest compression the resistance of QTC can fall from about 10^{12}–10^{13} Ω to less than 1 Ω, an exceptionally large dynamic range for a property of a solid material at room temperature [91]. When compressed into the low resistance state these composites can carry large currents without observable damage. Robot hands with QTC based tactile sensors have also been reported in literature [92, 93].

5.3.2.2 Conductive Polymer Composites with Conductive Polymer Fillers

There has been a growing interest in the intrinsic conductive polymers (ICP) due to their good electrical properties. Examples of these polymers include polypyrrole (PPy), polythiophene (PTh) and polyaniline (PANI) [94]. These polymers are either used as fillers in composites or coated on textiles. The modification of fibers and yarn using conductive polymers is an interesting approach for obtaining "intelligent textiles". Conductive fibers and yarn are discussed is a separate section later in this

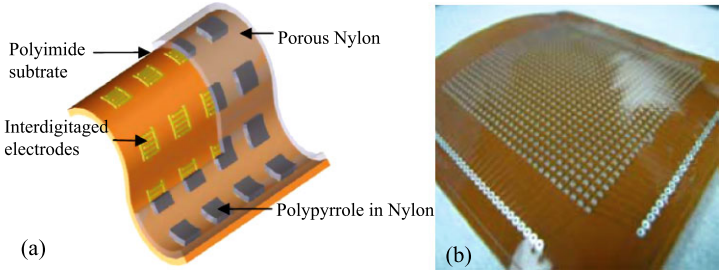

Fig. 5.14 (**a**) The schematic of porous nylon–polypyrrole composites based flexible tactile sensing array; (**b**) The 32 × 32 array realized on polyimide substrate (with permission from [95], ©(2008) IEEE)

chapter. The examples of tactile sensors based on composites with ICP fillers include the 32 × 32 flexible tactile sensing arrays developed by Yu et al. [95]. The array consists of 32 × 32 sensing elements, each of which consists of interdigitated copper electrodes on a flexible polyimide (PI) film. The overall size of the array is 89.9 × 89.9 mm^2, the sensing element size is 1 mm × 1 mm size and the center–center distance between two sensing elements is 1.9 mm. The PI film is covered with porous nylon, to which polypyrrole fillers are electrochemically added. The fillers are added only on the pre-defined positions of interdigitated electrodes. The scheme and the fabricated tactile sensing arrays are shown in Fig. 5.14. The polypyrrole polymers (electrical conductivity in the range 500–7500 S/cm) form electrically conductive paths in the porous nylon. These conductive paths are shortened when external pressure is applied and as a result the resistance decreases. An interesting aspect of this sensor is that more conductive paths are formed in the absence of conductive materials such as water. This property allows using the same sensor to measure contact pressure/force and also the moisture sensation. The flexible tactile sensor has stable sensitivity ($\Delta R/R_0$) of 0.1%/kPa for pressure up to 30 kPa. Another example of composites with conductive polymer fillers is the strain sensor by Flandlin et al. [94]. The strain sensing material is obtained by mixing an insulating latex of styrene-butyl acrylate copolymer with a colloidal suspension of polypyrrole. Since elastomer molecules as a matrix can be more thoroughly mixed with the conductive polymer, the composites made from them offer an attractive alternative for sensing applications.

5.3.2.3 Conductive Polymer Composites with Carbon Microcoils Fillers

Tactile sensors using composites with uniformly distributed carbon microcoils (CMCs) fillers in the silicone matrix have been proposed by Chen et al. [96]. The carbon microcoils have a three dimensional spiral structure with 10–15 μm diameter. Obtained by the Ni catalyzed pyrolysis of acetylene, these microcoils can be stretched up to 5–10 times their original lengths. The changing *LCR* (inductance, capacitance and resistance) parameters of the CMCs (increase with extension and

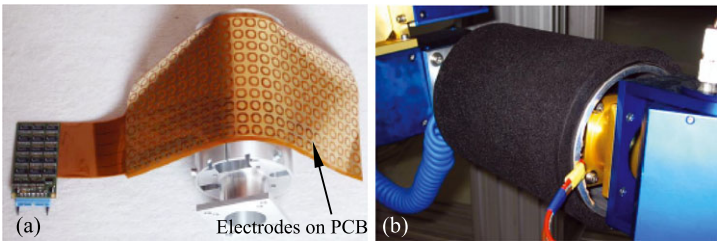

Fig. 5.15 The tactile sensor system based on graphite–elastomer composites; (**a**) The base of flexible sensor array on PCB; (**b**) The electrodes on the sensor array covered with graphite–elastomer composite. The tactile sensing arrangement is integrated on the forearm of a robotic hand (with permission from [98], ©(2003) IEEE)

decrease with contraction) is used to detect the applied force. The micro tactile elements, $80 \times 80 \times 80\ \mu m^3$ in size, have high sensitivity of 0.3 mgf (1 Pa) and response time of the order of milliseconds.

5.3.2.4 Conductive Polymer Composites with Graphite Nanosheet Fillers

Conductive graphite filler based composites present another alternative for tactile sensors. Composites with graphite nanosheet fillers (diameters ranging from 5–20 μm and thickness from 30–80 nm) incorporated in to poly(methyl methacrylate) (PMMA), polystyrene (PS), nylon 6, and silicone rubber have been reported in literature [97]. In each case only a slight amount of graphite nanosheet (about 1.0 vol %) is sufficient to satisfy the critical percolation transition. The advantage of lesser amount of graphite fillers is that the satisfactory electrical properties are achieved without compromising the mechanical properties of the composite. The graphite nanosheet–silicone rubber composite with 1.36 vol % of graphite nanosheet exhibits a much stronger and reversible positive piezoresistive effect. The change of electrical resistance is many orders of magnitude of pressing and a high sensitivity of the finger-pressure range. An implementation of graphite–elastomer composites for robotic tactile sensing system is reported by Kerpa et al. [98]. The sensor, shown in Fig. 5.15 consists of a 10×23 array of electrodes on a printed circuit board (PCB) which is covered with a few millimeters thick foam made of cellular rubber–graphite fillers composite. The overall size of tactile array is 175 mm × 376 mm and the spatial resolution of the sensors is 15 mm. The wiring is done on the PCB. Under pressure the resistance between the foam and the electrodes changes and this change is measured via the electrodes. The electrodes are selected via multiplexers and the corresponding signal is forwarded to a microcontroller, where signal is digitized, locally pre-processed, and converted in to a serial data stream. The serial data stream is transferred via CAN bus to the main control PC. The tactile sensor by Kerpa et al. [98] requires loading for at least 20 seconds before precise pressure can be measured. A common issue with conductive composites is that the creep of polymer matrix results in the time dependence of the composite resistance. The graphite

filler based composites are thus not completely free from such issues, even if their performance in this regard is better than other composites [97].

5.3.2.5 Conductive Polymer Composites with Carbon Black Fillers

Carbon black, an amorphous form of carbon, is another material which is widely used as a conductive filler. Carbon black with only small diameter and large surface area are suitable as the filler to improve electric conductivity. An example of carbon black based sensors includes the low cost solution for thin (0.125 mm) and flexible pressure sensor array by Wang et al. [99]. The sensing element uses conductive carbon black powder and vulcanized liquid silicone rubber as conductive filler and insulating matrix, respectively in the mass ratio of 0.08:1. The sensing array consists of nine sensing elements, formed at the intersections of rows and columns electrodes. The rows and column electrodes have been realized on opposite surfaces of the composite. On application of force, the gap between carbon black particles is reduced and they touch or come close to each other—leading to the formation of local conductive path due to contact effect or tunneling effect. The change is resistance is thus gives a measure of applied pressure. Another similar tactile sensing scheme, based on carbon black filler based composites, is used in the prototype of DLR touch sensor by Strohmayr et al. [100]. However, in this case the conductive composites have been obtained by blending the ultra-soft Poly[styrene-b-(ethylene-cobutylene)-b-styrene] (SEBS) polymers with carbon black filler material. Using carbon black as an additive to achieve electrical conductivity usually requires a concentration so high that it will increase the melt viscosity and decrease the mechanical properties of the polymers. One of the recent trends to overcome this drawback is to use multiphase polymer blends and hence reduce the overall carbon black concentration [101].

5.3.2.6 Conductive Polymer Composites with Carbon Nanotube Fillers

Carbon nanotubes (CNT) are interesting materials for designing highly sensitive tactile devices, owing to their electrical and electromechanical properties. They are highly conductive as well as super compressive, both of which make them highly pressure sensitive material [102]. Like graphite fillers, the nanocomposites with aligned CNTs have significantly small percolation threshold (three order of magnitude lower than conventional particulate carbon-black fillers [103]), implying that the conductivity of composite will rise monotonically over a long range of strain. This also means that satisfactory electrical properties can be achieved without compromising the mechanical properties of the composite. The performance (sensitivity, resolution, dynamic range etc.) of tactile sensors using pressure sensitive elastomers can therefore be significantly improved by replacing conventional carbon-black filler with CNTs.

A comparison of composites with carbon black filling and multi-walled carbon nanotube (MWNT) by Engel et al. [104] shows an 8-fold improvement in sensitivity

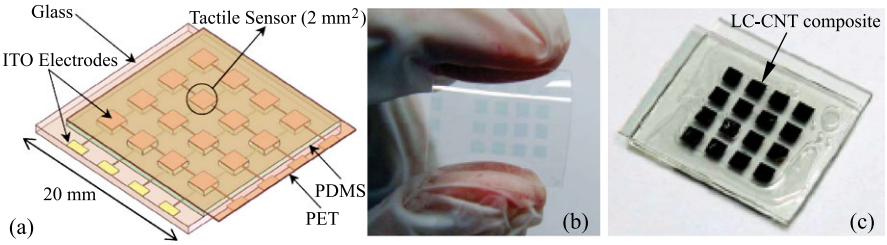

Fig. 5.16 A carbon nanotube–liquid crystals composite based tactile sensor array. (**a**) The schematic of the sensing array; (**b**) The ITO (Indium tin oxide) electrodes of the array on PET; (**c**) The fabricated 4 × 4 tactile sensing array (with permission from [107], ©(2011) IEEE)

through the use of MWNT. Furthermore, a comparison between MWNT blended polydimethylsiloxane (PDMS) and polyurethane (PU) elastomers shows that the former exhibits a lower percolation threshold (approximately 2% versus 10% in PU). Using PDMS–MWNT composite in a capacitive tactile sensor in place of the non-conductive PDMS capacitors can result in an improved performance. For example, the PDMS–MWNT composite based capacitive tactile sensor by Engel et al. [104] has linear output i.e. change in capacitance above 19 kPa load (below this load the response is not linear) and the sensitivity 1.67%/kPa. The sensitivity is more than twice the sensitivity of a non-conductive PDMS (0.7%/kPa [105]) capacitor. Simple CNT based flexible tactile sensing structures for measuring normal and shear forces have been developed by Hua et al. [106]. Depending on the sensor structure, the reported range of sensitivities (i.e. change in resistance per unit force) for normal (from 0 to 6 N) and shear forces (from 0 to 0.10 N) are 0.49%/N to 22.76%/N and 18%/N to 95%/N respectively.

A 4 × 4 tactile sensing array based on liquid crystal (LC)–CNT composites by Lai et al. [107] is shown in Fig. 5.16. The sensing material of each tactile sensor consists of the LC–CNT composite (MWCNT:LC concentration 0.01:1), a deformable PDMS elastomeric structure, an ITO glass substrate and an ITO PET film. An interesting aspect of this tactile sensing arrangement is that the sensing ranges can be tuned by varying the magnitude of the applied external field (supplied by the array scanning circuitry).

Various CPC materials, and tactile sensing solutions based on them, discussed above present a low cost alternative for robotic tactile sensing with interesting properties like mechanical flexibility. As such the field of CPC based sensors is still nascent and therefore, faces a set of challenges. Some of the major concerns include temperature and chemical stability, long term stability, performance shift over time, creep, relaxation, hysteresis, and tolerance to high electric field [108]. For example, the resistance of nanocomposite elastomers may incur changes in the presence of changes in stress/strain, temperature, humidity, and chemical environment. The cross talk is a primary issue for sensor applications. Due to the degradation and the non-linearities, elastomers/composites are not suited for accurate absolute force measurements, but they are good enough for force distribution measurements, which

is not affected by the non-linearities. The advancements in the processing technologies and improvements in material properties of CPCs will help solve many of above challenges—eventually allowing integration of CPCs semiconductors, and the underlying electronics collectively to be used as hybrid sensors and almost complete tactile system.

5.3.3 Conductive Fibers, Yarns and Intelligent Textiles

For years the textile industry has been weaving metallic yarns into fabrics for decorative purposes. However, recently it is the new generation of fibers, fabrics and the intelligent textiles produced from them, that has been attracting considerable attention. Conductive materials such as conductive fibers, yarns, coatings and ink, etc. have been used in intelligent textiles for a range of applications including sensing, electrostatic discharge, welding of plastics, electromagnetic interference shielding, data transfer in clothing, as well as military applications like camouflage and stealth technology. Smart or intelligent textiles using fabric-based sensors to monitor gesture, posture or respiration have been exploited in many applications. The idea for the most intelligent or smart textile is to used conductive fibers as transmission lines to connect the sensors and other technological components attached to the textile like embroidery. The textile transmission line consists of conductive yarns integrated into a flexible textile base. Conductive yarns are either pure metal yarns or composites of metals and non-conductive textile materials that help improve mechanical properties. Conductive fibers coated with sensitive material (e.g. piezoresistive material) are also used as sensors. Depending upon different applications, several sensing segments can be embedded into textiles such that distributed strains can be measured with the sensors. The conductive and semiconductive yarns can also be used to further improve the intelligent textile based sensors systems by building reliable transistors with well-defined electrical properties using them. Examples of conductive and semiconductive yarns topology, proposed by Bonfiglio et al., to build transistors are given in Fig. 5.17 [109]. When inserted in a fabric, this can be seen as an elementary network where purely metallic “drain” (D) and “source” (S) wires cross the yarn-like transistor indicated with “gate” (G). Current advances in new materials, textile technologies, and miniaturized electronics make wearable systems more feasible.

5.3.4 Polymer Gels and Fluids

A gel consist of an elastic cross linked network and a fluid filling the interstitial spaces of the network. The network of long polymer molecules holds the liquid in place and so gives the gel what solidity it has. Gels are wet and soft and look like a solid material but are capable of undergoing large deformation. The polymer gels

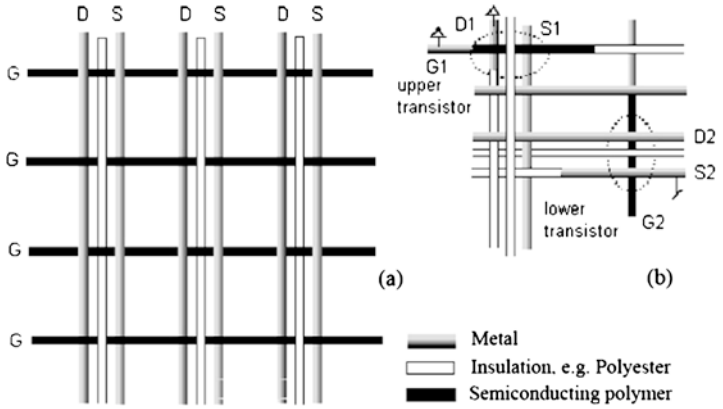

Fig. 5.17 The electronic devices in yarn textile topology. (**a**) The transistor array structure. GS represents textile ribbons with the gate contact and the organic semiconductor; (**b**) The ring oscillator structure to implement different conductivity properties (insulating, metal, semiconductor) on the same yarn (with permission from [109], ©(2005) IEEE)

induce a spontaneous ionization on mechanical compression. The potential in gels is produced by the chemical free energy of the polymer network[7] [110]. Soft touch sensors can be obtained using polyelectrolyte gels. The polyelectrolyte gels induce a spontaneous ionization on mechanical compression and thus electrical potential as large as a few millivolts is produced. They also exhibit reverse piezoelectric effect, i.e. an applied potential causes the gel to swell visibly. Using this phenomenon, Sawahata et al. [111] constructed a simple touch sensor capable of lighting a photo diode array according to the amplitude of mechanical deformation. The fact that human tissue is also composed of electrolytic materials with very similar mechanical properties suggests intriguing possibilities for new designs of sensing fingers.

A weakly conductive fluid based tactile sensing arrangement that mimics the mechanical properties and distributed touch receptors of the human fingertip is presented by Wettels et al. [112]. The sensing structure consists of a rigid core surrounded by a weakly conductive fluid contained within an outer elastomeric skin. Multiple electrodes are mounted on the surface of the rigid core and connected to impedance-measuring circuitry, embedded within the core itself. On contact, the outer elastomeric layer is deformed, leading to deformation of the fluid path around the electrodes, which eventually results in a distributed pattern of impedance changes. The resulting impedance pattern given an indication about the forces (e.g. magnitude and direction) and the objects (e.g. shape, hardness/softness) that ap-

[7] When a piece of weak polyelectrolyte gel is pressed, the pH of the gel changes reversibly. The pH change is associated with an enhanced ionization of the carboxyl groups under deformation. The compression in one direction expands the gel laterally and induces a one-dimensional dilatation of the polymer network in this direction. This brings about an increased chemical free energy (a decrease in entropy) of the polymer chain, which should be compensated for by a simultaneous increase in its degree of ionization.

plied them. The sensor system is able to detect forces ranging from 0.1–30 N that produce impedances ranging from 5–1000 kΩ. The factors affecting the sensitivity of this tactile sensor include, conductivity of the fluid, the viscoelastic properties of the combined system of skin and pressurized fluid, volume and pressure of fluid, and the material and geometry of the electrode contacts. It is generally desirable for the fluid to have a low viscosity to minimize damping and hysteresis, and a high resistivity so that the measured impedance of the series circuit (electrodes plus fluid) is dominated by the fluid resistance rather than the capacitive reactance of the metal–electrolyte interfaces. For these reasons, water with a low concentration of NaCl (1/12th the concentration of physiological saline) has been used by Wettels et al. [112].

The tactile sensors made of polymer gels and fluids have similarities with tactile perception in living organisms in a sense that the macroscopic deformation in both of them induces the ionic rearrangement that gives rise to a certain amount of transmembrane potential. Many of the features of gels, such as softness, wetness, and elasticity etc. are also similar to that of natural tissues. Because of these similarities, the gel based soft system may open new possibilities in the investigation of artificial tissue-like tactile perception for prosthetics and robotics.

5.3.5 Electro-Optic Materials and Sensors

In recent years, electro-optic[8] polymers (e.g. chromophores) and semiconductor nano-crystals (e.g. CdS, CdSe) have been used to make various optical and sensing devices due to several advantages, such as large and fast electro-optic (EO) response. The EO response of semiconductor nano-crystals is higher than that of response electro-optic polymers because of surface and quantum size effects. The semiconductors with their band gap in visible region of light spectrum are of interest as they emit visible light; hence their photoluminescence (and electroluminescence) is visible to human eye and can be imaged using a CCD. Group II–VI semiconductors such as cadmium sulfide (CdS), cadmium selinide (CdSe) and zinc sulfide (ZnS) are widely used materials in this regard.

A highly sensitive sensor using semiconductor nanoparticles, presented by Maheshwari and Saraf [50], is shown in Fig. 5.18. The sensor comprises of five nanoparticle monolayer structure separated by dielectric layers and it is constructed on transparent ITO electrodes by using layer-by-layer self-assembly technique (Fig. 5.18(a)). The organic dielectric layers, which as approximately 5–6 nm thick, are made of four alternating monolayers of poly(allylamine hydrochloride) (PAH) and poly(styrene sulfonate) (PSS). The sensor (2.5 cm^2 in size) works on the principle of electron tunneling. On application of bias voltage V across the film, the electric current flows through it and the CdS nanoparticles emit visible light at

[8]The electro-optic effect is the change in refractive index of materials with external field.

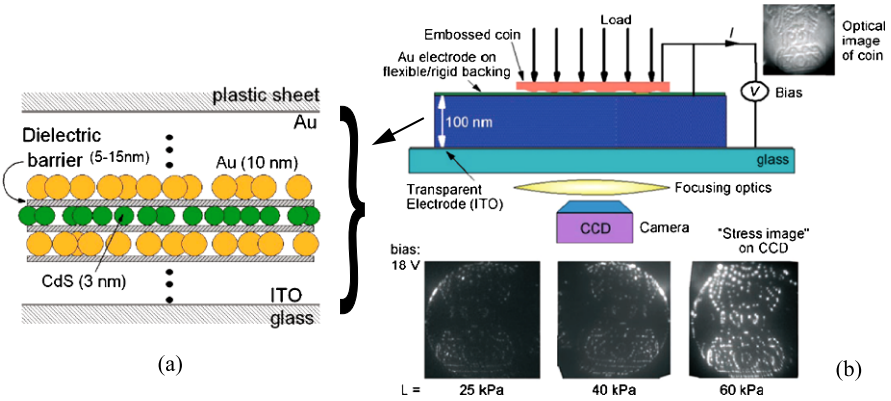

Fig. 5.18 A tactile sensor based on electro-optical device. (**a**) Schematic representation of the tactile sensor showing the nanoparticle monolayers spaced by organic dielectric layers; (**b**) The working of tactile sensor. Pressing a coin on the surface of the device generates its electroluminescence image on the CCD. The intensity of image increases with the load (Reproduced with permission from [19], Copyright Wiley-VCH Verlag GmbH & Co. KGaA)

a wavelength of 580 nm. When a load is applied to the top Au/plastic electrode (Fig. 5.18(b)), the dielectric layer is compressed and the particles are brought closer, facilitating the electron tunneling and thus causing an increase in both the local current density and the electroluminescent light. Thus, the device directly converts stress into electroluminescent light and modulation in local current density, both of which are linearly proportional to local stress. The change is electroluminescent light can be recorded on a digital camera, as in Fig. 5.18(b) and hence a high resolution image of the load can be obtained. The spatial resolution better than that of the human fingertip ($\sim$40 μm) can be obtained with the above approach.

A major concern with measuring the electroluminescent light is related to the increase in overall size of the sensing arrangement, as the CCD camera adds to the sensor size. This issue can be overcome by recording the stress distribution in terms of change in the local current density distribution. The current through a nanoparticle based tunneling device is exponentially sensitive to the magnitude of energy barrier between the nanoparticles and the physical distance between them. This means that the current can be modulated by increasing the electric field (voltage bias) across the nanoparticles (which increases the energy of the electrons and hence lowers the energy barrier) or by decreasing the barrier width by reducing the separation between the nanoparticles. Therefore, instead of measuring the electroluminescent light, the stress distribution can be obtained by measuring the local current density distribution (in a configuration similar to liquid-crystal display) [19]. Thus, above sensing device can also achieve high resolution without any optical components.

5.4 Tactile Sensor Structures

Various transduction methods and materials discussed in previous sections have been utilized in various tactile sensing structures. Some of these structures, such as microelectromechanical systems (MEMS), silicon transistors, printed circuit boards, and fabric etc. are discussed in this section.

5.4.1 MEMS Based Sensors

The MEMS based tactile sensors are obtained either by micromachining the silicon or by using the polymers. In general, they employ capacitive [113–118] or piezoresistive [28, 30, 119] mode of transduction. The early works on piezoresistive and capacitive micromachined sensors have produced arrays of force sensing elements using diaphragms or cantilevers as the sensing principle [120, 121]. The silicon-diaphragm based tactile sensors are dominated by piezoresistive sensing methods, even if the capacitive devices are an order of magnitude more sensitive. One of the reasons for this dominance could be that the capacitive sensing method, though very effective for measuring normal loads, is difficult to use when measuring shear loads—meaning that the method cannot be used practically for 3-D load detections. The piezoresistive devices also offer higher linearity. A few examples of the MEMS tactile sensing structures obtained using both the micromachined silicon and polymers are given below.

5.4.1.1 Si-MEMS Approach

The MEMS based tactile devices realized by silicon micromachining, are quite sensitive and result in higher spatial resolution. With a piezoresistive bridge arrangement on the sensing element, the MEMS based sensing devices can detect both the shear and normal components of applied stress. For example, the 64×64 element high resolution (≈ 300 μm) traction sensors array by Kane et al. [28] shown in Fig. 5.3(a) is composed of a central shuttle plate suspended by four bridges, with each of the four bridges containing a polysilicon piezoresistor. The strains in each of the bridges due to pure applied shear (σ_s) and normal (σ_n) stresses are given as [28]:

$$\varepsilon_s = \frac{b^2}{2\sqrt{2}(EA)}\sigma_s \tag{5.10}$$

$$\varepsilon_n = \frac{b^2 L}{2(EA)\delta}\sigma_n \tag{5.11}$$

where ε_s and ε_n are the shear and normal strains respectively; b is the shuttle plate width; (EA) is the overall axial stiffness of the bridge; L is the length of the bridge;

and δ is the normal deflection of the shuttle plate. This overall axial stiffness parameter (EA) is the sum of the products of the Young's moduli, E, and the cross-sectional area A, for each of the materials in the bridge. The equation (5.10) is obtained by assuming that the structural deformation is primarily the axial strain of the bridges. Further, the deflections are assumed to be small in calculating both normal and shear strains. Using each of the piezoresistors as the variable leg of a resistive half-bridge and by monitoring the intermediate node voltage of the half-bridge (by differentially comparing to the output of an off-chip voltage divider circuit that served as the second leg of a full Wheatstone bridge circuit), a measure of the strain (and hence applied stress) can be obtained as [28]:

$$V_i = \frac{kG(\varepsilon_{ni} + \varepsilon_{sxi} + \varepsilon_{syi})}{4} V_d \tag{5.12}$$

where V_i is the unamplified measurement node voltage for bridge i; ε_{ni} is the strain induced in bridge due to applied normal stress; ε_{sxi} is the strain due to the shear stress applied in the x-axis direction; ε_{syi} is the strain due to the shear stress applied in the y-axis direction; G is the piezoresistive gauge factor; V_d is the bridge drive voltage; and k is the amplification factor. Through differential addition of the four voltage signals (V_1, V_2, V_3, V_4), the independent voltage measures of the three components of an applied traction stress can be obtained as [28]:

$$T_n = [V_1 + V_2 + V_3 + V_4] = \frac{kV_d b^2 LG}{2(EA)\delta} \sigma_n \tag{5.13}$$

$$T_{sx} = [-V_1 - V_2 + V_3 + V_4] = \frac{kV_d b^2 G}{2\sqrt{2}(EA)} \sigma_{sx} \tag{5.14}$$

$$T_{sy} = [-V_1 + V_2 + V_3 - V_4] = \frac{kV_d b^2 G}{2\sqrt{2}(EA)} \sigma_{sy} \tag{5.15}$$

The above equation indicate that the measure of normal stress T_n and the shear stress components T_{sx} and T_{sy} are linear functions of the applied stresses and independent of the orthogonal stresses applied to the sensor. Following above equations the normal and shear stress sensitivities of the sensor by Kane et al. [28] are 1.59 mV/kPa (normal stress range 0–35 kPa) and 0.32 mV/kPa (shear stress range 0–60 kPa) respectively. The method similar as above has been adopted in many MEMS based tactile sensing schemes to obtain the normal and shear component of the applied force. One such example of polymer-MEMS based tactile sensor by Hwang et al. [122] is discussed below in this section.

The utility of MEMS based tactile sensing structures, realized by silicon micromachining, to practical robotic systems has been limited until now because of reasons like brittle nature of silicon. The MEMS based tactile sensors are unable to withstand large forces/pressure due to inherent fragile nature of the structure—even if the sensor is normally embedded or covered with an elastic covering. The packaging of MEMS based tactile sensors has also been a challenging issue. A few examples of silicon based piezoresistive force sensor that address the problems of robust packaging, small size and overload tolerance include the sensor by Beebe

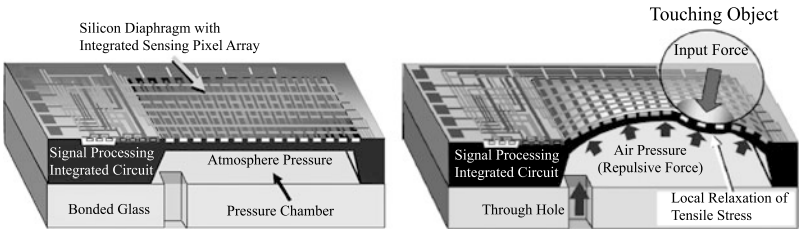

Fig. 5.19 (**a**) MEMS based tactile Image Sensor with piezoresistive pixels integrated on single-silicon diaphragm. (**b**) Pneumatically controlled flexible surface of diaphragm (with permission from [30], ©(2006) IEEE)

et al. [26]. The sensor measures the force (rather than pressure) applied to a 4 mm raised dome on the device surface. The device exhibits a linear response, good repeatability and low hysteresis, and has a flexible and durable packaging. In general, devices that incorporate brittle sensing elements such as silicon based diaphragms, including those embedded in protective polymers, have not proven to be reliable interfaces between a robotic manipulator and the manipulated object [49].

It is difficult to realize flexible tactile sensors through micromachining of brittle materials such as silicon. A novel method of obtaining MEMS based flexible tactile sensing structure has been reported by Takao et al. [30]. The sensing structure consists of a silicon diaphragm, with an array of 6×6 piezoresistive sensing elements on it and a pressure chamber beneath, as shown in Fig. 5.19. The diaphragm is swollen like a balloon by the pressurized air, provided to the chamber through the hole and hence the stiffness of the diaphragm is controlled by the air pressure. In this way, a force in the range of 2.1–17.6 gmf can be controlled by applying pressure in the range of 5–64 KPa. The extra provisions needed to supply and monitor the air are quite cumbersome and as such the arrangement is bulky. The alternative solutions explored to obtain flexible MEMS tactile sensors include using polyimide (PI) layers as a connecting material between silicon-diaphragm sensors, mounting silicon-diaphragm sensors on flexible printed circuit board substrates with a conductive epoxy etc. [123].

5.4.1.2 Polymer-MEMS Approach

Recently, a considerable effort is focused on the use of polymers in microelectronics systems and MEMS due to their potential for conformability. Polymers have been extensively used as both structural and functional materials for micro-devices. A number of examples given in previous section are related to the use of polymers (mainly, fibers and elastomers) as functional materials for tactile sensing. The discussion here primarily focuses on using polymers as structures and tactile sensing

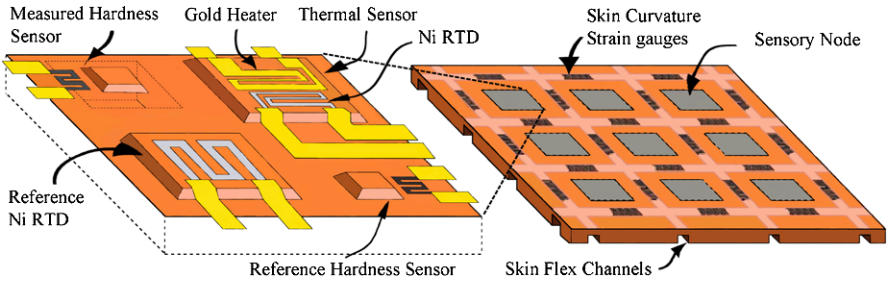

Fig. 5.20 (*left*) The scheme of a multimodal sensory node on polyimide substrate. (*right*) Distribution of sensing nodes on the flexible skin, (Reprinted from [124], ©(2005) with permission from Elsevier)

systems developed from them using MEMS approach. The polymer-MEMS[9] approach for developing tactile sensing structures has gained interest, partly because of the difficulty in obtaining a practical mechanically flexible system from silicon. The development of silicon-diaphragm-based tactile sensors requires both complex and expensive processes. A polymer-MEMS based process, on other hand, is a simple and low cost solution. Furthermore, unlike silicon micromachining the dimensions of the tactile sensing skin are not limited by the finite sizes of silicon wafers.

Multimodal polymer-MEMS based tactile sensor developed by Egnel et al. [124] is shown in Fig. 5.20. Realized on flexible polyimide (PI) substrate the sensor skin is capable of sensing the hardness, roughness, temperature and thermal conductivity of the object in contact. The skin is made on flexible polyimide sheet and consists of multiple sensor nodes arranged in an array format. Each node consists of four elements: a thermal conductivity measurement unit, a temperature measurement unit, and two membranes with metal strain gauges for measuring surface roughness and contact force. The two membranes also work in tandem to provide measurement of the hardness without knowledge of the contact force. The thermal conductivity measurement unit consists of a micro patterned metallic resistive heater and a thermal resistor. Electric current supplied to the resistive heater causes ohmic heat generation, which is transferred to a nearby temperature sensor (made of Ni) by thermal conduction via the substrate. The heat is sensed by the thermal resistor located 10–50 μm away. The steady-state read out of the thermal resistor is a function of the thermal conductivity of the object in contact, as it provides a parallel thermal conductive path. The two membranes with metal strain gauges use metallic strain gauge elements to detect strain developed in the polyimide substrate when the sensor is in contact with an object. The above sensing arrangement by Egnel et al. is a good attempt toward measuring multiple contact parameters other than force/pressure.

[9]Polymer-MEMS does not mean that the device is entirely made of polymers. In fact, heterogeneous integration of organic and inorganic materials is often necessary and desired. For example, it is often necessary to integrate signal conditioning and signal processing electronics directly with sensors. For large area sensor skin, the ability to integrate electronics and sensors is indispensable to reduce lead routing complexity.

However, utility of the sensor is limited by wiring complexity and the scalability of the wiring interconnects. Furthermore, the finished sensing arrangement does not contain signal processing electronics.

Another polymer-MEMS based tactile sensing arrangement, capable of detecting both normal and shear load, is presented by Hwang et al. [122]. The sensor is realized on PI and PDMS substrates and uses thin-film metal strain gauges for measuring 3-D forces. Unlike the tactile sensors obtained with micromachining of silicon, the sensor by Hwang et al. has no diaphragm like structures. When an external force is applied to the device, the thin metal film structure and the polymer incur a deformation that causes changes in the electric resistance. The sensor is capable of measuring normal loads up to 4 N. However, the sensitivity to shear loads is much lower. Furthermore, the sensor fails to discriminate between shear and normal loads when they are applied at same time. The changes in resistance corresponding to the magnitude and direction of applied force can be measured by connecting the strain-gauge in bridge arrangement similar to one described earlier in this section. The sensitivity of this type of tactile sensor is expected to be lower than that of the silicon-diaphragm based tactile sensors because: (a) the polymer substrates allow relatively small strain, and (b) the gauge factor of thin metal film used to make strain gauge is lower than that of polysilicon resistors.

5.4.2 Transistor Based Sensors

An interesting development in the field of sensing has been the use of electronic devices as sensors. For long, the electronic devices such as diodes and transistors have been used for measuring parameters like temperature and pH of solutions. In recent years, tactile sensing too has benefited from this development. Initially limited to the silicon transistor based arrangements (e.g. extended gates [125–127], and POSFET [128] etc.), the tactile sensing skin using organic transistors [34, 129] are being developed nowadays. The approach is particularly interesting, as it allows integrating the sensor and measurement circuit on same substrate and therefore opens up possibilities of performing the signal processing very close to the sensors. Besides improving the signal to noise ratio, the marriage of transducer and electronics will improve the force resolution, spatial resolution, signal to noise ratio, and has potential of reducing the number of wires, which is a key robotics issue. Some of these silicon and organic transistor based tactile sensing structures are presented below. A detailed discussion on silicon based extended gate tactile sensing arrays and high resolution POSFET tactile sensing arrays is presented in Part II of the book.

5.4.2.1 Silicon Transistor Based Tactile Sensors

The tactile sensors and sensing arrays have been developed using hybrid organic–inorganic structures such as coupling the piezoelectric polymers with the transistor.

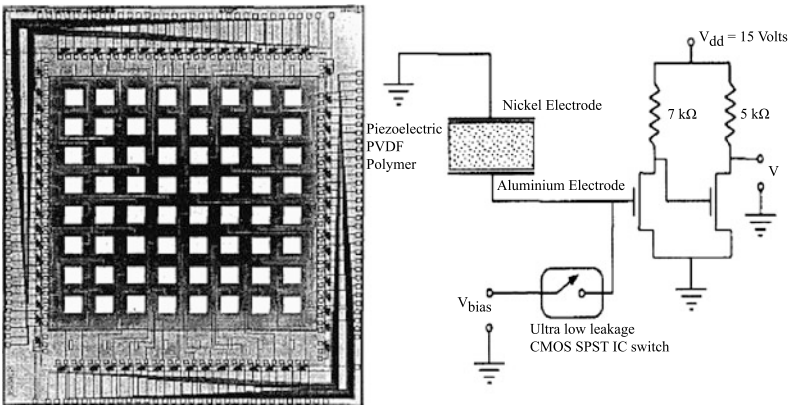

Fig. 5.21 (*left*) The tactile sensing array based on the extended gate approach. An 8 × 8, array of electrodes in the center, is surrounded by MOSFET devices on the periphery of the chip. (*right*) Schematic of a discrete in situ MOSFET amplifier (with permission from [83], ©(1996) IEEE)

The location, size and shape of the piezoelectric polymers in such cases may vary and accordingly the size and location of transistors too may differ. The two alternatives that have come to notice are: the tactile sensors using transistors having extended gates, and the conventional transistor with metal over the gate area only.

In the case of extended gate devices, the MOSFET is confined to a small portion of the cell area and gate metal is extended to occupy most of the cell. The extended gate electrode, which acts as a charge collector for the relatively small transistor, may be of arbitrary shape and size. The transducer material such as piezoelectric polymer (e.g. PVDF) is deposited over the extended gate electrode, which acts the lower electrode of the transducer. The electric charge resulting from piezoelectric action in the transducer will thus appear directly on the gate of the MOS transistor. The working principle is further described in Chaps. 6 and 7. As the MOSFET is an uncommitted circuit element, it may be used to provide amplification of this electrical signal or as a multiplexer to select for further processing one signal from many such transducer elements [130].

The tactile sensing array (overall size—9200 × 7900 μm) by Kolesar et al. [83, 125] is based on aforementioned extended gate approach. The 8 × 8 extended electrodes, shown in Fig. 5.21, act as the lower electrodes for the PVDF piezoelectric film. The PVDF film (40 μm thick) is epoxy adhered to the lower electrodes (dimension—400 × 400 μm). The lower/extended electrodes are thus capacitively coupled to the PVDF, via the insulating glue bond. An oxide layer on the surface of the silicon electrically isolates these electrode from the silicon. The extended gates are connected to the MOSFET devices located on the periphery of the chip. The spatial resolution of the array is less than 1 mm and response of tactile sensor is linear for loads spanning 0.8–135 gmf (0.008–1.35 N). A response bandwidth of 25 Hz has been achieved. The tactile sensing array also possesses simple amplifier circuitry (Fig. 5.21). The problem of response stability and reproducibility, associated with piezoelectric based tactile sensors, is taken care by a pre-charge bias technique.

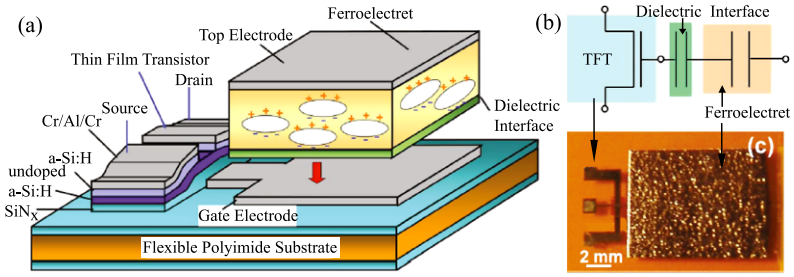

Fig. 5.22 (**a**) Sketch of the ferroelectret field effect transducer. The ferroelectret film is mechanically and electrically interfaced with the amorphous Si field-effect transistor via a thin dielectric coupling layer; (**b**) Equivalent circuit diagram; and (**c**) Photograph of one transducer element (Reprinted with permission from [126] ©[2006] American Institute of Physics)

The pre-charge bias feature incorporated in the sensor design (and operated by external circuitry), impresses a short-duration (0.1 seconds), low-level, direct current voltage ($V_{bias} = 2.5$ V) to the upper and lower electrodes of the PVDF film. The sensor is thus initialized before each cycle and eventually the voltage fluctuations is minimized.

Following a similar approach, a 32 element tactile sensing array, epoxy-adhered with 25, 50 and 100 μm piezoelectric polymer film (PVDF-TrFE) [127, 131], is presented in the next chapter. The touch sensing elements have been tested over a much wider range of dynamic forces (up to 5 N in the frequency range of 2 Hz–5 kHz) and a spatial resolution of 1 mm has been reported. With charge and voltage amplifiers, designed specifically for testing and discussed in Appendix C, the response of discrete sensing elements is found to be linear in above said test range. The use of the tactile sensing array for detecting objects based on their hardness has also been demonstrated.

Another example of extended gate approach is the sensor by Graz et al. [126] where ferroelectret material has been used as transducer. The ferroelectret material (made from 70 μm thick cellular polypropylene films) is epoxy adhered to the extended electrode of an amorphous silicon (a-Si:H) thin film transistor (TFT). As depicted in Fig. 5.22, the sensor has been realized on the a 50 μm thick polyimide film. The ferroelectrets can be used in capacitive and piezoelectric modes and accordingly the ferroelectret TFT sensor can be used to detect static and dynamic contacts. Other advantages of ferroelectrets are the large longitudinal piezoelectric signals and the corresponding negligible pyroelectric and transverse piezoelectric responses. This makes ferroelectrets insensitive to temperature drifts and device bending. However, due to lower charge carrier mobility the a-Si:H based transistor are much slower than the standard silicon transistors. Another example of extended gate transistor based tactile sensor, using zinc oxide (ZnO) as transducer is presented by Polla et al. in [132].

The extended gate approach brings the sensor and analog sensors frontend closer and hence overall response is better than that of conventional approach, where the sensor and analog sensors frontend are separated by some distance. One problem

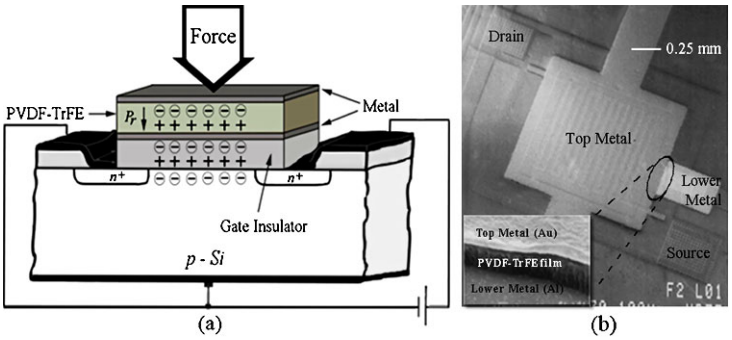

Fig. 5.23 (**a**) The structure and working of a POSFET touch sensing device; (**b**) SEM image of a POSFET device. The cross section of piezoelectric polymer film is shown in *inset*

with the extended gate structures (realized on silicon) is the capacitance between the extended gate electrode and the conductive silicon wafer, with the insulating oxide layer acting as a dielectric. Because of the limitations of IC technology, the oxide layer is usually much thinner (≈1.5 μm) than the piezoelectric film. With a dielectric constant comparable to that of the PVDF, the oxide capacitance will be much larger than that of the PVDF. This means the oxide layer may result in a significant reduction of overall sensitivity and increases the propagation delay [60]. Thus, benefits of closely located sensor and electronics are not fully exploited with extended gate approach. Such effects can be reduced by depositing the piezoelectric polymer film on the gate area of the transistor itself, as explained in following para and later in Chaps. 7 and 8.

The issues such as negative effect of the large oxide capacitance introduced by the extended gates, can be overcome by depositing the piezoelectric material on the gate ares of the transistor. This is precisely what is done in case of POSFET touch sensing devices that are described in detail in Chaps. 7 and 8. However, for completing the discussion, POSFET tactile sensing devices are briefly described here. The structure of a POSFET touch sensing devices is shown in Fig. 5.23 [128]. It can be noticed that the piezoelectric polymer film is present over the gate area of the MOS device. Thus, transducer material is an integral part of a POSFET device. The structure of POSFET device is similar to that of metal-ferroelectric-metal-insulator-semiconductor type FeRAM (Ferroelectric Random Access Memory) devices [133], which are used for memory applications. However, working of POSFET devices is fundamentally different from that of FeRAM—as former responds to changes in mechanical stimulus and the output in latter results from electric field switching. The remanent polarization (P_r) of the polarized polymer and the principle of charge neutrality lead to the appearance of fixed charges $\pm Q$, as shown in Fig. 5.23. For piezoelectric polymers in thickness mode, as in this work, the mechanical stress T_3, electric field E_3 and electric displacement D_3 are related as [61]:

$$D_3 = d_{33} \times T_3 + \varepsilon_{33} \times E_3 \tag{5.16}$$

where, d_{33} and ε_{33} are the piezoelectric and dielectric constants of piezoelectric polymer respectively. Following (5.16), the electric displacement can be controlled either by varying the electric field E_3 and/or by the mechanical stress T_3 (or the contact force). While former is used in FeRAM to switch the polarization state, latter is used in the POSFETs (and also in extended gate devices) to modulate the charge in the induced channel of underlying MOS device. Thus, the (contact) force variation is directly reflected as variation in the channel current of POSFET devices—which can be further processed by an electronic circuitry that may also be integrated on the same chip. It should be noted that silicon based devices are also known to exhibit piezoresistive effect i.e. their resistivity changes due to applied stressed. This raises an important question about the source of the change in channel current—piezoelectric action of P(VDF-TrFE) polymer film present on the gate area or the piezoresistive behavior of silicon? The same argument holds for previous discussed extended gate devices. In practice, both piezoelectric and piezoresistive effects contribute. As demonstrated by Dahiya et al. in [128], the contribution of piezoresistive effect is about 1% of the total output and therefore the change in the channel current of a POSFET (and hence its output) is primarily because of the piezoelectric action of the P(VDF-TrFE) polymer film. However, the same may not be true in case of flexible transistors which experience large piezoresistive effect due to large bending.

The POSFET tactile sensing devices are very sensitive with recorded sensitivity of more than 100 mV/N [134, 135]), have spatial resolution of about 1 mm and linear response to normal dynamic forces ranging from 0.01 N to 5 N [128, 135] with frequencies up to 2 kHz. Unlike extended gate approach, the POSFETs occupy lesser area on the chip. The silicon real estate thus saved can be used to accommodate on-chip electronics and signal processing circuitry. The local processing of the tactile signal will also help reduce the amount of tactile data transferred to higher perceptual levels of a robot. A detail discussion on POSFET tactile sensing devices and the tactile sensing chips made from them later is given in Chaps. 7 and 8.

5.4.2.2 Organic Transistor Technology Based Sensors

A few notable tactile sensing structures reported in literature are based on organic field effect transistors (OFETs) [34, 129]. The OFET based tactile sensing solutions have the advantage of being mechanically flexible, low cost solution, relative ease of fabrication and easy implementation over large areas. As presented earlier in this chapter, the OFETs can also be implemented in yarn textile topology, making wearable electronics more real [109]. The examples of OFETs based tactile skin include the 32×32 pressure sensing array by Someya et al. [34]. Realized on ultra-high heat-resistant and mechanically flexible poly(ethylene naphthalate) (PEN) substrate (thickness 100 μm), the sensing structure and its equivalent circuit are shown in Fig. 5.24. The OFET is based on pentacene and pressure conductive rubber is employed as the transducer. Unlike previously discussed transistor based tactile sensors (where transducer is connected to gate terminal), in this case the pressure sensitive

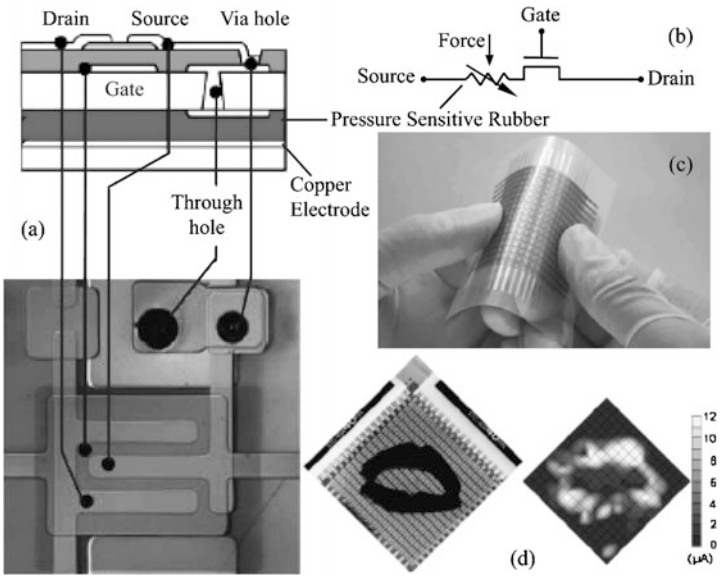

Fig. 5.24 (**a**) The section and top view of the organic FET sensing element with pressure sensitive rubber; (**b**) Equivalent circuit of the sensing element; (**c**) The 16 × 16 OFET array; (**d**) A pressure image of a kiss mark taken with the presented sensors (with permission from [34], ©(2004) National Academy of Sciences, USA)

rubber is placed in the source–drain path. The applied pressure results in a resistance change of the pressure conductive rubber, which in turn results in a change in the current I_{ds} flowing between the source and drain. The applied pressure is thus modulates I_{ds}, which can be easily measured using external circuitry. In a sense the OFET technology has been used as the readout element for the pressure conductive rubber. The applied pressure in the range 0 to 30 kPa ($\approx$ 300 gmf/cm^2) results in the resistance variation from 10 MΩ to 1 kΩ. The sensing elements have a pitch of 2.54 mm. In this study, the cycle time of each transistor is around 30 milliseconds, from which the total time to access 16 × 16 transistors is estimated to be 480 milliseconds if one word line is read at the same time. These figures are quite high with respect to the tactile sensing structures based on silicon technology and as such the sensors are suitable for slow varying (quasi static) mechanical stimuli.

Another OFET based tactile sensing structure is presented by Mannsfeld et al. [129]. In this arrangement, a pyramid structured highly pressure sensitive PDMS thin film is employed as the dielectric over the gate area of a rubrene based OFET (on PET substrates).[10] On application of pressure, the PDMS is compressed and the

[10]There is an analogy between this structure and the human skin. The pyramid like microstructure can be viewed similar to the intermediate ridges present at the dermis–epidermis junction of human skin (Chap. 3). The ridge microstructures in skin are also known to improve the tactile sensitivity in humans [136–138].

dielectric capacitance changes (due to reduction in thickness), eventually resulting in a change of the source–drain current (I_{ds}) of the transistor. Since the transducer is placed on the gate area, the structural arrangement is similar to the previously discussed POSFET touch sensing devices. However, in this case the channel current is modulated by change in dielectric capacitance. In case of POSFET, the channel current is primarily modulated by the change in polarization level of the piezoelectric polymer film. The response of this tactile sensing arrangement to the application of pressure is non-linear, which is expected due to the fact that in OFETs the source-drain current (I_{ds}) linearly depends on the dielectric capacitance but the PDMS film capacitance has non non-linear dependence on the pressure. By using 6×6 μm^2 pyramid-structured PDMS film, Mannsfeld et al. demonstrated the improvements in sensitivity of the dielectric material. The maximum slope of the relative capacitance change of the pyramidal PDMS film in the 0.2 kPa range is 0.55 kPa^{-1}. This is about 30 times higher than the sensitivity of unstructured film in the same range. The loads as low as 3 Pa have been detected. The microstructured PDMS also results in an improved relaxation time of the transducer. The structured films relaxed on the millisecond timescale, and unstructured films relaxed over times as long as 10 s, which is about 10^4 times slower. This means the transducer will again be ready for use in few milliseconds after the load is removed. However, the overall response time depends on both the transducer and the transistor and in this context the slow response of OFET remains a concern.

A major drawback of the OFET based tactile sensing arrangements is that their overall speed of response is slow. For instance, the response time of above described pentacene based OFET by Someya et al. [34] is 30 milliseconds. With further lower charge carrier mobility (1.0 cm^2/V.s as compared to 1.4 cm^2/V.s in [34]) the rubrene based OFET by Mannsfeld et al. [129] is expected to be more slower. From the point of view tactile sensing, the overall response depends on both transducer and the OFET. As far as transducer is concerned, the response speed can be improved by using a material that responds faster. Consider for instance, the pressure sensitive rubber used by Someya et al. [34] typically has the response time of the order of hundreds of milliseconds. Replacing pressure sensitive rubber with polymers like PVDF can significantly improve the response speed. Sometimes, shaping the transducer suitably can also result in improved response speed. For instance, a structured PDMS film can respond faster that an unstructured film. The above discussed tactile sensing arrangement by Mannsfeld et al. [129] is one such example. Comparing the response of an unstructured PDMS film with a structured PDMS film (having two dimensional arrays of square pyramid microstructures), Mannsfeld et al. noted that although the response to an external load (15 kPa) was immediate in both films, the relaxation times were quite disparate. The structured films relax on the millisecond timescale, and unstructured films relaxing over times as long as 10 seconds, which is about 10^4 times slower. The lengthy response time of unstructured PDMS films severely limits their usefulness as pressure sensors. Unfortunately, not many alternatives are available for improving the response speed of the organic transistors. It is well known that the mobility of organic semiconductors is about three orders of magnitude lower than that of silicon, which makes them much slower than the standard silicon based devices [139] and hence issue of overall slow response remains.

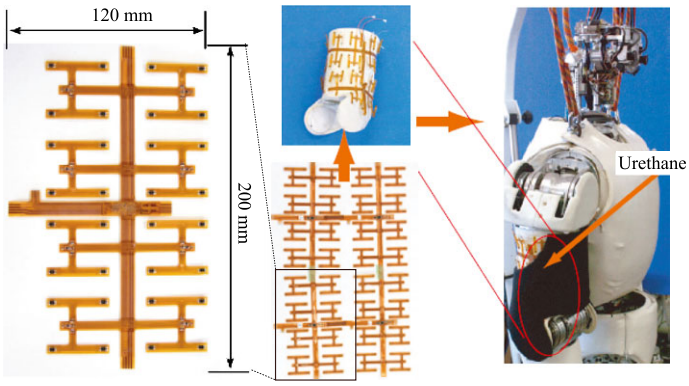

Fig. 5.25 A lightweight, conformable and scalable large area skin on flexible printed circuit board (with permission from [46], ©(2006) IEEE)

Other issues with organic devices are that they typically have short life and their operational stability is influenced by various factors, including dependence on stress voltage and duty cycle, gate dielectric, environmental conditions, light exposure, and contact resistance [140].

The tactile sensing arrays based on organic semiconductor technology cannot attain (at least in the present state of the technology) the high-speed performance exhibited by their silicon counterparts, but, features like physical flexibility and the low cost of fabrication make them good candidates for large-area skin. As presented in Chap. 3, the spatio-temporal requirements are not same for all body parts. For body parts such as belly and back (that make a large portion of the body) the spatio-temporal requirements are not high. Same argument when applied to robotics (e.g. humanoids), the organic transistor based solutions can be useful in future for less sensitive parts.

5.4.3 Sensors on Flexible Substrates

This concluding section presents the flexible tactile sensing structures realized on flexible substrates (sensor is not necessarily flexible), which is normally the flexible printed circuit board (PCB). As argued in previous chapter, for better integration and effective utilization of tactile data, the tactile sensing schemes are required to be conformable. In this context, many tactile sensing structures have been realized on flexible PCBs. Generally, these structures employ off-the-shelf sensing and electronics components. It is difficult to discuss all such solution and therefore only a selected few (having sensing component based on different transduction methods) with an aim to cover large area of a robot's surface are discussed below.

A conformable and scalable large area tactile sensing skin, having pressure sensing elements based on optical mode of transduction, is shown in Fig. 5.25. As discussed earlier in this chapter, each touch element on this tactile skin by Ohmura et

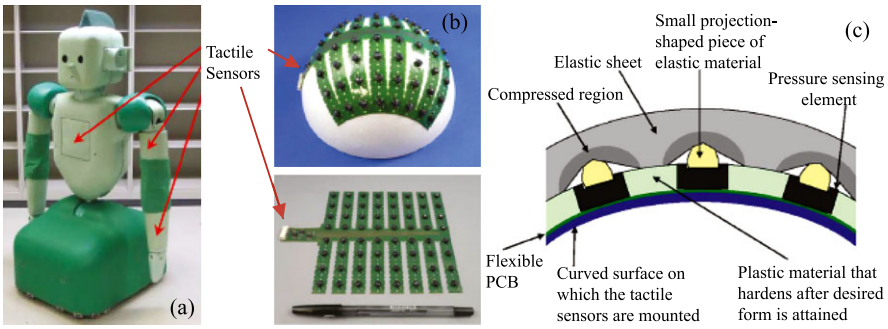

Fig. 5.26 The tactile skin structure with piezoresistive pressure sensors distributed on a flexible printed circuit board. (**a**) The location of tactile sensor on the humanoid robot RI-MAN; (**b**) The comb-shaped sensor patch; (**c**) Sensor embedded in elastic sheet (with permission from [11], ©(2008) IEEE)

al. [46] consists of photo-reflectors (3.2 mm × 1.1 mm × 1.7 mm) under the urethane foam (thickness 5 mm) and the light scattered by urethane foam upon deformation gives the measure of mechano-electrical transduction. The foam thickness controls the dynamic range and sensitivity of the sensors. The sensor sheet (120 mm × 120 mm) is lightweight (1.7 gram) and consists of 32 tactile sensing elements, one micro-controller and four serial bus terminators mounted on a flexible substrate. This modular skin can be folded and cut and the sensor coverage is adjustable via the addition/deletion of the modules. A couple of tactile sensor sheets are integrated to obtain a larger tactile sensor sheet (of 120 tactile sensor elements) and the final sheet is mounted on the arm of a humanoid robot is shown in Fig. 5.25. Time to scan one sensor element is 0.2 milliseconds (the interval between the instant when host computer sends the address packet until receiving the sensor data) and spatial resolution is approximately 3 cm. The sensing elements communicate via serial bus. To overcome the difficulties associated with serial bus for real-time communication at high speed, a ring-type network is proposed. The serial busses are connected with slave nodes of a custom designed ring-type network, with each node having a small-sized microcontroller as a serial-bus master. One major disadvantage of this scheme is the large current consumption by LEDs (∼50 mA per sensing element). To overcome this problem Ohmura et al. have proposed scanning control scheme, whereby the number of powered-on LEDs are restricted through time-sharing control. As the control is time-shared, the analog to digital converters and the analog signal wires can also be shared. The current in each LED can also be controlled through pulse width modulation. In fact, the same can also be employed to tune the sensitivity of the tactile sensing elements. Other concern related to this approach stems from the fact that urethane foam used in sensing element inevitably causes strong hysteresis and creep.

Another tactile sensing scheme on flexible printed circuit board, presented by Mukai et al. [11], is shown in Fig. 5.26. The piezoresistive semiconductor pressure sensors have been distributed on comb-shaped printed circuit board and embedded

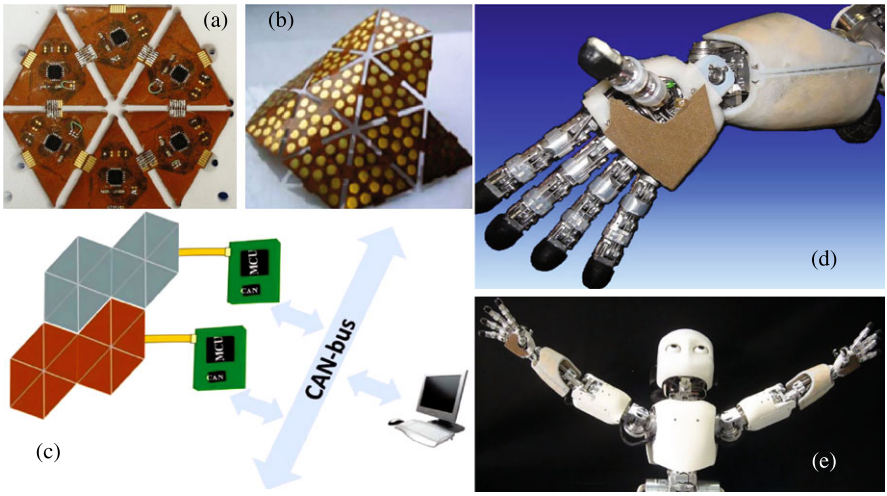

Fig. 5.27 The conformable triangular modules on flexible PCB. (**a**) The back side of the sensor patch based on capacitive technology (sensors on other side); (**b**) The flexibility of structure, owing to triangular shape of modules and the flexible PCB; (**c**) The scheme for making large networked structure; (**d**) Implementation of sensors patch on hand of humanoid robot iCub; (**e**) Humanoid robot iCub with equipped with the sensor patches (with permission from [141], ©(2011) IEEE)

in an elastic sheet (5 mm thick). Each sensor sheet (comb-shaped PCB) has an array of 8×8 pressure-sensing elements with an 18 mm pitch. The piezoresistive semiconductor pressure sensors can detect the absolute pressure between 0.434–4.46 kgf/cm^2. These sensors have been employed because they have little hysteresis or creep and accuracy is better (though soft cover introduces some hysteresis and creep). The skin specifications target the sensing capabilities of a human when carrying another human in his/her arms (0–20 mm spatial resolution and 0.434–4.46 kgf/cm^2 pressure range, similar respectively to the human palm and 20×20 cm^2 of arm contact while holding a 60 kg human). All the wiring is concentrated into a comb-shaped region. The complete sampling of one tactile sensor patch with 8×8 elements requires about 15 ms, which is not always sufficient for the tactile feedback control. The sensor sheets cover the arms and chest of the 158 cm tall humanoid "RI-MAN" with a total of 320 pressure-sensing elements.

The capacitive technology based conformable sensor patches have been presented by Maggiali et al. [43]. The implementation of these patches is shown in Fig. 5.27(a), (b). Each triangular shaped modules, realized on flexible printed circuit board, contains 12 round pads on which capacitive pressure sensors are present and a capacitance-to-digital converter (AD7147 from Analog Devices [42]). A thick elastic sheet (silicone foam, 3–5 mm thick) covers the skin patch, allowing limited degree of compliance. However, it also adds to the challenges related to sensor calibration and drift in the response. The communication port on all three sides of triangle facilitates communication with adjacent modules—enabling creation of a large networked structure, as shown in Fig. 5.27(c). The signals from touch sen-

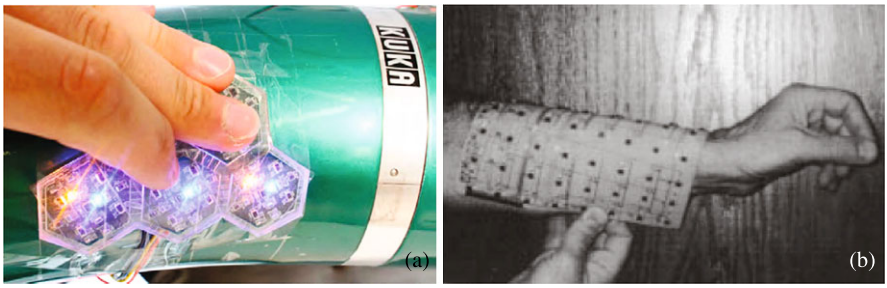

Fig. 5.28 Skin modules with proximity sensors. (**a**) The multimodal HEX-O-SKIN modules mounted on a KUKA lightweight arm (with permission from [142], ©(2011) IEEE); (**b**) The sensitive skin module on Kaptan substrate. The module uses 8×8 infrared sensors pairs (LEDs and detectors) as proximity sensors (with permission from [143], ©(2001) IEEE)

sors are sent to a microcontroller using I^2C serial bus communication interface. The sensor patch has low power consumption ($\sim$5 watts/m^2). This technology has been employed to cover large body parts of robots like iCub (Fig. 5.27(d), (e)), KASPAR and NAO [141]. The transducers and signal conditioning electronics wrap the robot surface, with components like microcontroller units installed in the inner body.

A vast majority of sensing structures are capable of detecting and measuring either contact force or pressure. The contact parameters are however not just limited to the contact force or pressure. There is a need to have sensing modules with multiple types of sensor to detect multiple contact parameters. The multimodal hexagonal shaped tactile sensing modules (HEX-O-SKIN), presented by Mittendorfer and Cheng [142] and shown in Fig. 5.28(a), are interesting in this context. The modules, implemented on printed circuit board, are equipped with multiple discrete sensors for temperature, acceleration, and proximity to emulate the human sense of temperature, vibration and soft or light touch respectively. Each module comprises of seven temperature sensors, three acceleration sensors and four proximity sensors. The modules, each weighing less than 2 grams, are embedded into elastomeric material to introduce limited degree of conformability.

Proximity or light touch sensing can be important for safe interaction. Covering of a manipulator with proximity sensing elements distributed all over it and their effective use in motion planning was first demonstrated in [8] and later followed in [9, 10, 143]. As shown in Fig. 5.28(b), distributed proximity sensing elements based on optical transduction were used as touch sensors in these works. Five sensor modules—each with 16 sensor pairs, consisting of a photo transistor and an IRLED were used. The distance between neighboring pairs is 25 mm. Scanning time of each module was 20 ms (serial access within a module), which was also the scanning time of all five modules (parallel access among modules). Thus a speed higher than that of PUMA robot velocity commands update rate (36 ms) was obtained and hence the data from sensing arrays could easily fit into the real-time operations performed by manipulator. The IRLEDs used in this work, were primarily used as proximity sensors and real contact with the sensor was avoided. But, a realistic situation would require safe interaction of robot while touching the objects. Nonetheless, for

Table 5.3 Tactile sensing arrays for parts like fingertips with high density receptors [28, 30, 40, 45, 83, 113–115, 127, 132, 144–154]

Year	Author	Transduction Method	Miniaturization Technique	No.of Sensing Element	Spatial Res. (mm)	Signal Condition Circuit	Sensor BW (kHz)	Range of Force^{+} (N)/Pressure* (kPa)	Force/ Pressure Sensitivity
1984	Raibert et al.	Resistive	Si-micromachining	6 × 8	∼0.6	Yes[a]	–	–	–
1985	Polla et al.	Piezoelectric	Si-micromachining	8 × 8	0.07	Yes[a]	–	2^{+}	5.2 mV/gm
1988	Suzuki et al.	Capacitive	Si-micromachining	32 × 32	0.5	No	–	0.01^{+}	0.45 pF/g
1990	Sugiyama et al.	Piezoresistive	Si-micromachining	32 × 32	0.25	Yes[a]	60	–	0.02 mV/kPa
1993	Liu et al.	Piezoresistive	Si-micromachining	4 × 4	1	Yes[a]	–	200*	0.032 mV/kPa
1994	Audet et al.	Magnetic	Si-micromachining	–	–	Yes	–	–	–
1996	Chu et al.	Capacitive	Si-micromachining	3 × 3	2.2	No	–	0.01^{+}	0.13 pF/g (nf) 0.32 pF/g (shf)
1996	Gray et al.	Capacitive	Si-micromachining	8 × 8	0.1	No	–	$1.0 \times 10^{-4+}$	20 µN
1996	Kolesar et al.	Piezoelectric	Si-micromachining	8 × 8	0.7	Yes[a]	0.025	$0.008–1.35^{+}$	–
1997	Desouza et al.	Capacitive	Si-micromachining	16 × 16	500 dpi	No	–	–	100 µN
2000	Kane et al.	Piezoresistive	MEMS on Si	64 × 64	0.3	Yes[a]	–	35*	1.59 mV/kPa
2000	Leineweber et al.	Capacitive	Si-micromachining	8 × 1	0.24	Yes[a]	–	100–300*	13.5 mV/kPa
2002	Castelli	Capacitive	–	8 × 8	>2	No	–	120*	–
2002	Hellard et al.	Optical	–	4 × 4	>1	No	–	–	–
2003	Wen et al.	Field Emission	MEMS on Si	8 × 8	1	Yes[a]	–	150*	30.1 mV/kPa
2005	Choi et al.	Resistive & Piezoresistive	–	24	∼1	No	–	2^{+}	–
2006	Okha et al.	Optical	–	–	2	No	–	2^{+}	1 mN
2006	Schmidt et al.	FSR & Capacitive	–	1_{static} $16_{dyn.}$	–	No	∼0.003 35	$0.05–10^{+}$ $<0.01^{+}$	5 mN
2006	Takao et al.	Piezoresistive	MEMS on Si	6×6	0.42	Yes[a]	–	$0.021–0.176^{+}$	0.5–1 V/N
2009	Dahiya et al.	Piezoelectric	Si-micromachining	32	1	Yes	5	5*	0.5 V/N
2010	Dahiya et al.	Piezoelectric	Si-micromachining	5×5	1	Yes	2.13	5*	0.5 V/N

[a]Electronics circuitry (partly) on the sensing array; nf—Normal force; shf—Shear force

Table 5.4 Tactile sensing arrays for parts like large area skin with low density of receptors [8, 10, 11, 25, 34, 43, 46, 49, 67, 124, 155, 156]

Year	Author	Transduction Method	Miniaturization Technique	No.of Sensing Element	Spatial Res. (mm)	Signal Condition Circuit[a]	Sensor BW (kHz)	Range of Force$^+$ (N)/Pressure* (kPa)	Force/ Pressure Sensitivity
1989	Cheung et al.	Optical	–	16	–	Yes	–	–	–
1992	Domenici et al.	Piezoelectric	On Polyimide	6 × 7	2.5	No	–	–	–
1992	Lumelsky et al.	Optical	–	500		Yes			
1998	Um et al.	Optical	–	1000	25	Yes	–	–	–
2004	Someya et al.	FSR	Organic FET	32 × 32	2.54	No	0.003	30*	–
2004	Weiss et al.	Resistive	–	3 × 8	4	No	–	–	–
2005	Engel et al.	Resistive	MEMS on Polymer	25	∼5	No	–	–	–
2005	Shan et al.	Piezoresistive	MEMS on Si	4 × 4	10	No	–	2$^+$	228 mV/N (nf) 34 mV/N (shf)
2006	Heo et al.	Optical	–	3 × 3	5	No	–	5 N	1 mN
2006	Kim et al.	Strain Gauge	MEMS on Polymer	4 × 4	2.5	No	–	0.6$^+$	0.52 V/N (nf) 0.25 V/N (shf)
2006	Ohmura et al.	Optical	–	8 × 4	∼30	No	–	–	–
2008	Maggiali et al.	Capacitive	Flexible PCB	12	10	Yes	–	–	–
2008	Mukai et al.	Piezoresistive	Flexible PCB	8 × 8	18	Yes	0.1	128*	–

[a]Electronics circuitry (partly) on the sensing array; nf—Normal force; shf—Shear force

first time it was demonstrated that motion planning can be done with no a priori knowledge about the environment (or dynamic environment).

5.5 Summary

A wide spectrum of tactile sensing technologies ranging from single tactile sensor elements to arrangements suitable for large areas have been discussed in this chapter. Some of the sensing arrangements reported in literature are grouped in Tables 5.3 and 5.4—mainly on the basis of their reported spatial resolution. The touch sensing arrays in Table 5.3 are suitable for high sensor density body locations like the fingertips and those in Table 5.4 are suitable for low density sensory body locations like palm, belly, etc. Current trend is to develop tactile sensing structures with mechanical/physical features like flexibility, stretchability etc. to cover various body parts of a robot. Sensor coverage that is continuous, and spanning the entire robot body, is desired for many robotic applications including the safe and effective robot operation. A growing interest can be found for tactile sensing schemes able to detect multiple contact parameters and the fusion of different tactile sensors data to detect multiple contact parameters. It is noted that packaging and integration of tactile sensing solutions with the robot has received a considerable attention. Encapsulation of sensor elements, wires and the integration of processing and communication hardware directly on to flexible PCBs are steps in this direction. Recent developments in materials chemistry, nano-structures, nano-devices, and single-molecule devices have great potential in improving the current technology. Current methods using a pressure sensitive elastomer can be significantly improved by replacing conventional fillers such as carbon-black with fillers like carbon nano tubes. An interesting aspect of some nano-materials based devices is their relatively low cost of fabrication, processing under ambient conditions and the ability to directly make large-area devices on curved surfaces. It is noted that the tactile sensor technology has reached quite a level of maturity and now it is also the time to consider important issues like interface electronics, the techniques to handle the tactile data and take out useful information from it, as otherwise potential technological benefits will make little sense for robotics.

References

1. L.D. Harmon, Automated tactile sensing. Int. J. Robot. Res. **1**(2), 3–31 (1982)
2. H.R. Nicholls, M.H. Lee, A survey of robot tactile sensing technology. Int. J. Robot. Res. **8**(3), 3–30 (1989)
3. W.D. Hillis, Active touch sensing. Int. J. Robot. Res. **1**(2), 33–44 (1982)
4. P. Dario, D. de Rossi, Tactile sensors and gripping challenge. IEEE Spectr. **22**(8), 46–52 (1985)
5. S.C. Jacobsen, I.D. McCammon, K.B. Biggers, R.P. Phillips, Design of tactile sensing systems for dextrous manipulators. IEEE Control Syst. Mag. **8**, 3–13 (1988)

6. R.D. Howe, M.R. Cutkosky, Dynamic tactile sensing: perception of fine surface features with stress rate sensing. IEEE Trans. Robot. Autom. **9**, 140–151 (1993)
7. R.D. Howe, Tactile sensing and control of robotics manipulation. Adv. Robot. **8**, 245–261 (1994)
8. E. Cheung, V.L. Lumelsky, Proximity sensing in robot manipulation motion planning: system and implementation issues. IEEE Trans. Robot. Autom. **5**(6), 740–751 (1989)
9. E. Cheung, V.L. Lumelsky, A sensitive skin system for motion control of robot arm manipulators. Robot. Auton. Syst. **10**, 9–32 (1992)
10. D. Um, B. Stankovic, K. Giles, T. Hammond, V.L. Lumelsky, A modularized sensitive skin for motion planning in uncertain environments, in *IEEE International Conference on Robotics and Automation*, Leuven, Belgium (1998), pp. 7–112
11. T. Mukai, M. Onishi, T. Odashima, S. Hirano, Z. Luo, Development of the tactile sensor system of a human-interactive robot "RI-MAN". IEEE Trans. Robot. **24**(2), 505–512 (2008)
12. Roboskin Project (2010). Available at: http://www.roboskin.eu/
13. R.S. Dahiya, G. Metta, M. Valle, G. Sandini, Tactile sensing—from humans to humanoids. IEEE Trans. Robot. **26**, 1–20 (2010)
14. R.S. Dahiya, G. Metta, G. Cannata, M. Valle, Guest editorial special issue on robotic sense of touch. IEEE Trans. Robot. **27**, 385–388 (2011)
15. B.V. Jayawant, Tactile sensing in robotics. J. Phys. E, Sci. Instrum. **22**, 684–692 (1989)
16. M.H. Lee, H.R. Nicholls, Tactile sensing for mechatronics—a state of the art survey. Mechatronics **9**, 1–31 (1999)
17. M.E.H. Eltaib, J.R. Hewit, Tactile sensing technology for minimal access surgery—a review. Mechatronics **13**, 1163–1177 (2003)
18. J. Dargahi, S. Najarian, Advances in tactile sensors design/manufacturing and its impact on robotics applications—a review. Ind. Robot **32**, 268–281 (2005)
19. V. Maheshwari, R. Saraf, Tactile devices to sense touch on a par with a human finger. Angew. Chem., Int. Ed. Engl. **47**, 7808–7826 (2008)
20. P. Puangmali, K. Althoefer, L.D. Seneviratne, D. Murphy, P. Dasgupta, State-of-the-art in force and tactile sensing for minimally invasive surgery. IEEE Sens. J. **8**, 371–381 (2008)
21. M.R. Cutkosky, R.D. Howe, W. Provancher, Force and tactile sensors, in *Springer Handbook of Robotics*, ed. by B. Siciliano, O. Khatib (Springer, Berlin, 2008), pp. 455–476
22. D. De Rossi, E.P. Scilingo, Skin-like sensor arrays, in *Encyclopedia of Sensors*, vol. X, ed. by C.A. Grimes, E.C. Dickey, M.V. Pishko (American Scientific Publishers, Valencia, 2006), pp. 1–22
23. P. Svyatoslav, Touch screen control and calibration—four-wire, resistive. Application Note AN2173, Cypress Microsystems (2004)
24. H. Zhang, E. So, Hybrid resistive tactile sensing. IEEE Trans. Syst. Man Cybern., Part B, Cybern. **32**(1), 57–65 (2002)
25. K. Weiss, H. Worn, Tactile sensor system for an anthropomorphic robotic hand, in *IEEE International Conference on Manipulation and Grasping*, Genoa, Italy (2004)
26. D.J. Beebe, A.S. Hsieh, D.D. Denton, R.G. Radwin, A silicon force sensor for robotics and medicine. Sens. Actuators A, Phys. **50**, 55–65 (1995)
27. M.R. Wolffenbuttel, P.P.L. Regtien, Polysilicon bridges for the realization of tactile sensors. Sens. Actuators A, Phys. **A2**(1–3), 257–264 (1991)
28. B.J. Kane, M.R. Cutkosky, G.T.A. Kovacs, A traction stress sensor array for use in high-resolution robotic tactile imaging. J. Microelectromech. Syst. **9**(4), 425–434 (2000)
29. FSR Sensors, Interlink Electronics Inc. (2008). Available at: http://www.interlinkelectronics.com
30. H. Takao, K. Sawada, M. Ishida, Monolithic silicon smart tactile image sensor with integrated strain sensor array on pneumatically swollen single-diaphragm structure. IEEE Trans. Electron Devices **53**(5), 1250–1259 (2006)
31. M. Shimojo, A. Namiki, M. Ishikawa, R. Makino, K. Mabuchi, A tactile sensor sheet using pressure conductive rubber with electrical-wires stitched method. IEEE Sens. J. **4**(5), 589–596 (2004)

32. H. Liu, P. Meusel, G. Hirzinger, A tactile sensing system for the DLR three-finger robot hand, in *International Symposium on Measurement and Control in Robotics* (1995), pp. 91–96
33. M.A. Diftler, R. Platt Jr., C.J. Culbert, R.O. Ambrose, W.J. Bluethmann, Evolution of the NASA/DARPA robonaut control system, in *IEEE International Conference on Robotics and Automation* (2003), pp. 2543–2548
34. T. Someya, T. Sekitani, S. Iba, Y. Kato, H. Kawaguchi, T. Sakurai, A large-area, flexible pressure sensor matrix with organic field-effect transistors for artificial skin applications. Proc. Natl. Acad. Sci. USA **101**(27), 9966–9970 (2004)
35. H. Alirezaei, A. Nagakubo, Y. Kuniyoshi, A highly stretchable tactile distribution sensor for smooth surfaced humanoids, in *7th IEEE-RAS International Conference on Humanoid Robots*, Pittsburgh, USA (2007)
36. Y. Kato, T. Mukai, T. Hayakawa, T. Shibata, Tactile sensor without wire and sensing element in the tactile region based on EIT method, in *IEEE Sensors Conference* (2007), pp. 792–795
37. D.S. Tawil, D. Rye, M. Velonaki, Improved image reconstruction for an EIT-based sensitive skin with multiple internal electrodes. IEEE Trans. Robot. **27**(3), 425–435 (2011)
38. Peratech Ltd., UK Patent PCT/GB98/00206 (WO 98/33193) Available at: http://www.peratech.co.uk
39. H.-K. Lee, S.-I. Change, E. Yoon, A flexible polymer tactile sensor: fabrication and modular expandability for large area deployment. J. Microelectromech. Syst. **15**(6), 1681–1686 (2006)
40. P.A. Schmidt, E. Mael, R.P. Wurtz, A sensor for dynamic tactile information with applications in human–robot interaction & object exploration. Robot. Auton. Syst. **54**, 1005–1014 (2006)
41. RoboTouch (2007). Available at: http://www.pressureprofile.com
42. AD7147: CapTouch™ (2008). Available at: http://www.analog.com
43. M. Maggiali, G. Cannata, P. Maiolino, G. Metta, M. Randazzao, G. Sandini, Embedded tactile sensor modules, in *11th Mechatronics Forum Biennial International Conference*, Limerick, Ireland (2008)
44. Available at: http://www.soton.ac.uk/~rmc1/robotics/artactile.htm
45. M. Ohka, H. Kobayashi, J. Takata, Y. Mitsuya, Sensing precision of an optical three-axis tactile sensor for a robotic finger, in *15th International Symposium on Robot and Human Interactive Communication "RO-MAN"* (2006), pp. 214–219
46. Y. Ohmura, Y. Kuniyoshi, A. Nagakubo, Conformable and scalable tactile sensor skin for curved surfaces, in *IEEE International Conference on Robotics and Automation*, Orlando, Florida, USA (2006)
47. E.M. Reimer, L. Danisch, Pressure sensor based on illumination of a deformable integrating cavity. U.S. Patent 5,917,180 (1999)
48. H. Yussof, J. Takata, M. Ohka, Measurement principles of optical three-axis tactile sensor and its application to robotic fingers system, in *Sensors: Focus on Tactile, Force and Stress Sensors*, ed. by J.G. Rocha, S. Lanceros-Mendez (I-Tech Publishers, Vienna, 2008), pp. 123–142
49. J.-S. Heo, J.-H. Chung, J.-J. Lee, Tactile sensor arrays using fiber Bragg grating sensors. Sens. Actuators A, Phys. **126**, 312–327 (2006)
50. V. Maheshwari, R. Saraf, High-resolution thin-film device to sense texture by touch. Science **312**, 1501–1504 (2006)
51. J. Winger, K.-M. Lee, Experimental investigation of a tactile sensor based on bending losses in fiber optics, in *Proceedings of the IEEE International Conference on Robotics and Automation*, Raleigh, North Carolina, USA (1988), pp. 754–759
52. J.-S. Heo, J.-Y. Kim, J.-J. Lee, Tactile sensors using the distributed optical fiber sensors, in *Proceedings of the 3rd International Conference on Sensing Technology* (2008), pp. 486–490
53. T.J. Nelson, R.B. Van Dover, S. Jin, S. Hackwood, G. Beni, Shear-sensitive magnetoresistive robotic tactile sensor. IEEE Trans. Magn. **Mag-22**(5), 394–396 (1986)
54. W.C. Nowlin, Experimental results on Bayesian algorithms for interpreting compliant tactile sensing data, in *IEEE International Conference on Robotics and Automation*, Sacramento,

California, USA (1991)
55. E. Torres-Jara, I. Vasilescu, R. Coral, A soft touch: compliant tactile sensors for sensitive manipulation. Technical report, CSAIL, Massachusetts Institute of Technology (2006)
56. E. Torres-Jara, Sensitive manipulation. Ph.D. thesis, Massachusetts Institute of Technology (2007). http://hdl.handle.net/1721.1/36371
57. R.-C. Luo, F. Wang, Y. Liu, An imaging tactile sensor with magnetorestrictive transduction, in *Robot Sensors*, vol. 2, ed. by A. Pugh (Springer, Berlin 1985), pp. 113–122
58. S. Ando, H. Shinoda, Ultrasonic emission tactile sensing. IEEE Control Syst. Mag. **15**(1), 61–69 (1995)
59. S. Ando, H. Shinoda, A. Yonenaga, J. Terao, Ultrasonic six-axis deformation sensing. IEEE Trans. Ultrason. Ferroelectr. Freq. Control **48**(4), 1031–1045 (2001)
60. R.S. Dahiya, M. Valle, G. Metta, L. Lorenzelli, POSFET based tactile sensor arrays, in *IEEE ICECS'07: The 14th International Conference on Electronics, Circuits and Systems*, Marrakech, Morocco (2007), pp. 1075–1078
61. R.S. Dahiya, M. Valle, L. Lorenzelli, Spice model of lossy piezoelectric polymers. IEEE Trans. Ultrason. Ferroelectr. Freq. Control **56**(2), 387–396 (2009)
62. S. Omata, Y. Murayama, C.E. Constantinou, Real time robotic tactile sensor system for the development of the physical properties of biomaterials. Sens. Actuators A, Phys. **112**(2–3), 278–285 (2004)
63. G.M. Krishna, K. Rajanna, Tactile sensor based on piezoelectric resonance. IEEE Sens. J. **4**(5), 691–697 (2004)
64. H. Shinoda, K. Matsumoto, S. Ando, Tactile sensing based on acoustic resonance tensor cell, in *Proceedings of TRANSDUCERS 1997, International Conference Solid-State Sensors and Actuators* (1997), pp. 129–132
65. K. Nakamura, H. Shinoda, A tactile sensor instantaneously evaluating friction coefficients, in *Proceedings of TRANSDUCERS 1997, International Conference Solid-State Sensors and Actuators* (1997), pp. 1430–1433
66. J. Dargahi, M. Parameswaran, S. Payandeh, A micromachined piezoelectric tactile sensor for an endoscopic grasper—theory, fabrication and experiments. J. Microelectromech. Syst. **9**(3), 329–335 (2000)
67. C. Domenici, D. De Rossi, A stress-component-selective tactile sensor array. Sens. Actuators A, Phys. **13**, 97–100 (1992)
68. P. Dario, G. Buttazzo, An anthropomorphic robot finger for investigating artificial tactile perception. Int. J. Robot. Res. **6**(3), 25–48 (1987)
69. K. Hosoda, Y. Tada, M. Asada, Anthropomorphic robotic soft fingertip with randomly distributed receptors. Robot. Auton. Syst. **54**, 104–109 (2006)
70. A.M. Taylor, D.M. Pollet, A. Hosseini-Sianaki, C.J. Varley, Advances in an electrorheological fluid based tactile array. Displays **18**, 135–141 (1998)
71. R.M. Voyles, G. Fedder, P.K. Khosla, Design of a modular tactile sensor and actuator based on an electrorheological gel, in *IEEE International Conference on Robotics and Automation*, USA, vol. 1 (1996), pp. 13–17
72. G.L. Kenaley, M.R. Cutkosky, Electrorheological fluid-based robotic fingers with tactile sensing, in *IEEE International Conference on Robotics and Automation*, USA, vol. 1 (1989), pp. 132–136
73. J.D. Carlson, S.P. Koester, Magnetically-controllable active haptic interface system and apparatus. U.S. Patent 6,283,859 B1
74. E.P. Scilingo, N. Sgambelluri, D. De Rossi, A. Bicchi, Haptic displays based on magnetorheological fluids: design, realization and psychophysical validation, in *The 11th Symposium on Haptic Interfaces for Virtual Environment and Teleoperator Systems (HAPTICS'03)* (2003), p. 10
75. Y. Liu, R.I. Davidson, P.M. Taylor, J.D. Ngu, J.M.C. Zarraga, Single cell magnetorheological fluid based tactile displays. Displays **26**, 29–35 (2005)
76. Pressure sensitive ink (2008). Available at: http://www.tekscan.com/

77. R. Kageyama, S. Kagami, M. Inaba, H. Inoue, Development of soft and distributed tactile sensors and the application to a humanoid robot, in *IEEE International Conference on Systems, Man, & Cybernetics*, vol. 2 (1999), pp. 981–986
78. K.B. Shimoga, A.A. Goldenberg, Soft materials for robot fingers, in *IEEE International Conference on Robotics and Automation*, Nice, France (1992), pp. 1300–1305
79. H.S. Nalwa, *Ferroelectric Polymers: Chemistry, Physics, and Applications* (Marcel Dekker, Inc., New York, 1995)
80. A.J. Lovinger, Ferroelectric polymers. Science **220**(4602), 1115–1121 (1983)
81. J.R. Flanagan, A.M. Wing, Modulation of grip force with load force during point-to-point arm movements. Exp. Brain Res. **95**, 131–143 (1993)
82. D. De Rossi, C. Domenici, Piezoelectric properties of dry human skin. IEEE Trans. Electr. Insul. **EI-21**(3), 511–517 (1986)
83. E.S. Kolesar, C.S. Dyson, R.R. Reston, R.C. Fitch, D.G. Ford, S.D. Nelms, Tactile integrated circuit sensor realized with a piezoelectric polymer, in *8th IEEE International Conference on Innovative Systems in Silicon*, Austin, Texas, USA (1996), pp. 372–381
84. B. Choi, H.R. Choi, S. Kang, Development of tactile sensor for detecting contact force and slip, in *IEEE/RSJ International Conference on Intelligent Robots and Systems* (2005), pp. 2638–2643
85. E.S. Kolesar, R.R. Reston, D.G. Ford, R.C. Fitch, Multiplexed piezoelectric polymer tactile sensor. J. Robot. Syst. **9**(1), 37–63 (1992)
86. Y. Yamada, T. Maeno, I. Fujimoto, T. Morizono, Y. Umetani, Identification of incipient slip phenomena based on the circuit output signals of PVDF film strips embedded in artificial finger ridges, in *SICE Annual Conference* (2002), pp. 3272–3277
87. R. Strümpler, J. Glatz-Reichenbach, Conducting polymer composites. J. Electroceram. **3**(4), 329–346 (1999)
88. D. Staufer, A. Aharony, *Introduction to Percolation Theory* (Taylor & Francis, London, 1992)
89. V.I. Roldughin, V.V. Vysotskii, Percolation properties of metal-filled polymer films, structure and mechanics of conductivity. Prog. Org. Coat. **39**, 81–100 (2000)
90. J.K.W. Sandler, J.E. Kirk, I.A. Kinloch, M.S.P. Shaffer, A.H. Windle, Ultra-low electrical percolation threshold in carbon-nanotube-epoxy composites. Polymer **44**(19), 5893–5899 (2003)
91. D. Bloor, K. Donnelly, P.J. Hands, P. Laughlin, D. Lussey, A metal-polymer composite with unusual properties. J. Phys. D, Appl. Phys. **38**, 2851–2860 (2005)
92. R. Walker, Developments in dextrous hands for advanced robotic applications, in *10th International Symposium on Robotics and Applications* (2004)
93. Shadow hand. Available at: http://www.shadowrobot.com
94. L. Flandin, G. Bidan, Y. Brechet, J.Y. Cavaille, New nanocomposite materials made of an insulating matrix and conductive fillers: processing and properties. Polym. Compos. **21**(2), 165–173 (2000)
95. S.-L. Yu, D.-R. Chang, L.-C. Tsao, W.-P. Shih, P.-Z. Chang, Porous nylon with electro-active dopants as flexible sensors and actuators, in *MEMS 2008. IEEE 21st International Conference on Micro Electro Mechanical Systems* (2008), pp. 908–911
96. X. Chen, S. Yang, M. Hasegawa, K. Kawabe, S. Motojima, Tactile microsensor elements prepared from arrayed superelastic carbon microcoils. Appl. Phys. Lett. **87** 054101, (2005)
97. L. Chen, G. Chen, L. Lu, Piezoresistive behaviour study on finger-sensing silicone rubber/graphite nanosheet nanocomposites. Adv. Funct. Mater. **17**, 898–904 (2007)
98. O. Kerpa, K. Weiss, H. Wörn, Development of a flexible tactile sensor system for a humanoid robot, in *IEEE/RSJ International Conference on Intelligent Robots and Systems*, Las Vegas, Nevada, USA (2003), pp. 1–6
99. L. Wang, T. Ding, P. Wang, Thin flexible pressure sensor array based on carbon black/silicone rubber nanocomposite. IEEE Sens. J. **9**(9), 1130–1135 (2009)
100. M.W. Strohmayr, H.P. Saal, A.H. Potdar, P. van der Smagt, The DLR touch sensor I: a flexible tactile sensor for robotic hands based on a crossed-wire approach, in *The 2010 IEEE/RSJ*

International Conference on Intelligent Robotics and Systems, Taipei, Taiwan (2010), pp. 897–903
101. J.-C. Huang, Carbon black filled conducting polymers and polymer blends. Adv. Polym. Technol. **21**(4), 299–313 (2002)
102. A.Y. Cao, P.L. Dickrell, W.G. Sawyer, M.N. Ghasemi-Nejhad, P.M. Ajayan, Super-compressible foam-like carbon nanotube films. Science **310**, 1307–1310 (2005)
103. J.K.W. Sandler, J.E. Kirk, I.A. Kinloch, M.S.P. Shaffer, A.H. Windle, Ultra-low electrical percolation threshold in carbon-nanotube-epoxy composites. Polymer **44**(19), 5893–5899 (2003)
104. J. Engel, J. Chen, N. Chen, S. Pandya, C. Liu, Multi-walled carbon nanotube filled conductive elastomers: materials and application to micro transducers, in *MEMS 2006: The 19th IEEE International Conference on Micro Electro Mechanical Systems*, Taipei, Taiwan (2006), pp. 246–249
105. B.S. Chiou, A.R. Lankford, P.E. Schoen, Modifying tubule distribution in tubule-filled composites by using polyurethane–polydimethylsiloxane interpenetrating polymer networks. J. Appl. Polym. Sci. **89**, 1032–1038 (2003)
106. H. Chia Hua, S. Wang-Shen, H. Chih-Fan, L. Chia-Min, F. Weileun, Y. Fu-Liang, A flexible, highly-sensitive, and easily-fabricated carbonnanotubes tactile sensor on polymer substrate, in *10th IEEE International Conference on Solid-State and Integrated Circuit Technology (ICSICT)*, Shanghai, China (2010), pp. 1388–1391
107. Y.-T. Lai, W.-C. Kuo, Y.-J. Yang, A tactile sensing array with tunable sensing ranges using liquid crystal and carbon nanotubes composites, in *The 24th IEEE International Conference on Micro Electro Mechanical Systems (MEMS)*, Cancun, Mexico (2011), pp. 553–556
108. C. Liu, Recent developments in polymer MEMS. Adv. Mater. **19**, 3783–3790 (2007)
109. A. Bonfiglio, D. De Rossi, T. Kirstein, I.R. Locher, F. Mameli, R. Paradiso, G. Vozzi, Organic field effect transistors for textile applications. IEEE Trans. Inf. Technol. Biomed. **9**(3), 319–324 (2005)
110. Y. Osada, J.-P. Gong, Soft and wet materials: polymer gels. Adv. Mater. **10**(11), 827–837 (1998)
111. K. Sawahata, J.P. Gong, Y. Osada, Soft and wet touch-sensing system made of hydrogel. Macromol. Rapid Commun. **16**, 713–716 (1995)
112. N. Wettels, V.J. Santos, R.S. Johansson, G.E. Loeb, Biomimetic tactile sensor array. Adv. Robot. **22**, 829–849 (2008)
113. B.L. Gray, R.S. Fearing, A surface micromachined microtactile sensor array, in *International Conference on Robotics and Automation*, Minneapolis, Minnesota, USA (1996)
114. Z. Chu, P.M. Sarro, S. Middelhoek, Silicon three-axial tactile sensor. Sens. Actuators A, Phys. **54**, 505–510 (1996)
115. M. Leineweber, G. Pelz, M. Schmidt, H. Kappert, G. Zimmer, New tactile sensor chip with silicone rubber cover. Sens. Actuators A, Phys. **84**, 236–245 (2000)
116. K. Suzuki, K. Najafi, K.D. Wise, A 1024-element high-performance silicon tactile imager. IEEE Trans. Electron Devices **37**(8), 1852–1860 (1990)
117. H.-K. Lee, S.-I. Chang, E. Yoon, A flexible polymer tactile sensor: fabrication and modular expandability for large area deployment. J. Microelectromech. Syst. **15**(6), 1681–1686 (2006)
118. U. Paschen, M. Leineweber, J. Amelung, M. Schmidt, G. Zimmer, A novel tactile sensor system for heavy load applications based on an integrated capacitive pressure sensor. Sens. Actuators A, Phys. **68**, 294–298 (1998)
119. M. Adam, E. Vazsonyi, I. Barsony, C.S. Ducso, Three dimensional single crystalline force sensor by porous Si micromachining, in *IEEE Sensors* (2004), pp. 501–504
120. M.R. Wolffenbuttel, P.P.L. Regtien, Design considerations for a silicon capacitive tactile cell. Sens. Actuators A, Phys. **A24**(3), 187–190 (1990)
121. M.R. Wolffenbuttel, P.P.L. Regtien, Polysilicon bridges for the realization of tactile sensors. Sens. Actuators A, Phys. **26**, 257–264 (1991)

122. E.-S. Hwang, J.-h. Seo, Y.-J. Kim, A polymer-based flexible tactile sensor for both normal and shear load detections and its application for robotics. J. Microelectromech. Syst. **16**(3), 556–563 (2007)
123. F. Jiang, G.-B. Lee, Y.-C. Tai, C.-M. Ho, A flexible micromachined based shear-stress sensor array and its applications to separation-point detection. Sens. Actuators A, Phys. **79**(3), 194–203 (2000)
124. J. Egnel, J. Chen, Z. Fan, C. Liu, Polymer micromachined multimodal tactile sensors. Sens. Actuators A, Phys. **117**, 50–61 (2005)
125. E.S. Kolesar, C.S. Dyson, Object imaging with a piezoelectric robotic tactile sensor. J. Microelectromech. Syst. **4**(2), 87–96 (1995)
126. I. Graz, M. Kaltenbrunner, C. Keplinger, R. Schwodiauer, S. Bauer, S.P. Lacour, S. Wagner, Flexible ferroelectret field-effect transistor for large-area sensor skins and microphones. Appl. Phys. Lett. **89**, 073501 (2006)
127. R.S. Dahiya, M. Valle, G. Metta, Development of fingertip tactile sensing chips for humanoid robots, in *5th IEEE International Conference on Mechatronics*, Malaga, Spain (2009), pp. 1–6
128. R.S. Dahiya, G. Metta, M. Valle, L. Lorenzelli, A. Adami, Piezoelectric oxide semiconductor field effect transistor touch sensing devices. Appl. Phys. Lett. **95**(3), 034105 (2009)
129. S.C.B. Mannsfeld, B.C.K. Tee, R.M. Stoltenberg, C.V.H.H. Chen, S. Barman, B.V.O. Muir, A.N. Sokolov, C. Reese, Z. Bao, Highly sensitive flexible pressure sensors with microstructured rubber dielectric layers. Nat. Mater. **9**, 859–864 (2010)
130. R.G. Swartz, J.D. Plummer, Integrated silicon-PVF2 acoustic transducer arrays. IEEE Trans. Electron Devices **26**(12), 1920–1932 (1979)
131. R.S. Dahiya, M. Valle, G. Metta, L. Lorenzelli, C. Collini, Tactile sensor arrays for humanoid robot, in *IEEE PRIME'07: The 3rd International Conference on Ph.D. Research in Microelectronics and Electronics*, Bordeaux, France (2007), pp. 201–204
132. D.L. Polla, W.T. Chang, R.S. Muller, R.M. White, Integrated zinc oxide-on-silicon tactile-sensor array, in *International Electron Devices Meeting* (1985), pp. 133–136
133. H. Ishiwara, Current status of ferroelectric-gate Si transistors and challenge to ferroelectric-gate CNT transistors. Curr. Appl. Phys. **9**, S2–S6 (2009)
134. A. Adami, R.S. Dahiya, C. Collini, D. Cattin, L. Lorenzelli, POSFET touch sensor with on-chip electronic module for signal conditioning, in *TRANSDUCERS 2011: The 16th IEEE International Conference on Solid-State Sensors, Actuators and Microsystem*, Beijing, China (2011), pp. 1982–1985
135. A. Adami, R.S. Dahiya, C. Collini, D. Cattin, L. Lorenzelli, POSFET touch sensor with CMOS integrated signal conditioning electronics. Sens. Actuators A, Phys. (2012). doi:10.1016/j.sna.2012.02.046
136. N. Cauna, Nature and functions of the papillary ridges of the digital skin. Anat. Rec. **119**, 449–468 (1954)
137. J. Scheibert, S. Leurent, A. Prevost, G. Debregeas, The role of fingerprints in the coding of tactile information probed with a biomimetic sensor. Science **323**, 1503–1506 (2009)
138. R.S. Dahiya, M. Gori, Probing with and into fingerprints. J. Neurophysiol. **104**, 1–3 (2010)
139. S.R. Forrest, The path to ubiquitous and low-cost organic electronic appliances on plastic. Nature **428**, 911–918 (2004)
140. S. Henning, Reliability of organic field-effect transistors. Adv. Mater. **21**, 3859–3873 (2009)
141. A. Schmitz, P. Maiolino, M. Maggiali, L. Natale, G. Cannata, G. Metta, Methods and technologies for the implementation of large-scale robot tactile sensors. IEEE Trans. Robot. **27**(3), 389–400 (2011)
142. P. Mittendorfer, G. Cheng, Humanoid multimodal tactile-sensing modules. IEEE Trans. Robot. **27**(3), 401–410 (2011)
143. V.L. Lumelsky, M.S. Shur, S. Wagner, Sensitive skin. IEEE Sens. J. **1**(1), 41–51 (2001)
144. R.J. De Souza, K.D. Wise, A very high density bulk micromachined capacitive tactile imager, in *IEEE International Conference on Solid-State Sensors and Actuators (TRANSDUCERS)*, Chicago, USA (1997), pp. 1473–1476

145. M.H. Raibert, An all digital VLSI tactile array sensor, in *IEEE International Conference on Robotics and Automation*, vol. 1 (1984), pp. 314–319
146. K. Suzuki, K. Najafi, K.D. Wise, A 1024-element high-performance silicon tactile imager, in *International Electron Devices Meeting* (1988), pp. 674–677
147. S. Sugiyama, K. Kawahata, M. Yoneda, I. Igarashi, Tactile image detection using a 1 K-element silicon pressure array. Sens. Actuators A, Phys. **A21–A23**, 397–400 (1990)
148. L. Liu, X. Zheng, L. Zhijian, An array tactile sensor with piezoresistive single-crystal silicon diaphragm. Sens. Actuators A, Phys. **32**, 193–196 (1993)
149. Y. Audet, G.H. Chapman, Design of a large area magnetic field sensor array, in *IEEE International Conference on Wafer Scale Integration*, San Francisco, USA (1994), pp. 272–281
150. F. Castelli, An integrated tactile-thermal robot sensor with capacitive tactile array. IEEE Trans. Ind. Appl. **38**(1), 85–90 (2002)
151. G. Hellard, A.R. Russell, A robust, sensitive and economical tactile sensor for robotic manipulator, in *Australian Conference on Robotics and Automation*, Auckland (2002), pp. 100–104
152. Z. Wen, Y. Wu, Z. Zhang, S. Xu, S. Huang, Y. Li, Development of an integrated vacuum microelectronic tactile sensor array. Sens. Actuators A, Phys. **103**, 301–306 (2003)
153. B. Choi, S. Kang, H. Choi, Development of fingertip tactile sensor for detecting normal force and slip, in *International Conference on Control, Automation and Systems*, Gyeong Gi, Korea (2005)
154. R.S. Dahiya, L. Lorenzelli, G. Metta, M. Valle, Development of fingertip tactile sensing chips for humanoid robots, in *IEEE-ISCAS 2010: The IEEE International Symposium on Circuits and Systems*, Paris, France (2010), pp. 1–4
155. J.H. Shan, T. Mei, L. Sun, D.Y. Kong, Z.Y. Zhang, L. Ni, M. Meng, J.R. Chu, The design and fabrication of a flexible three-dimensional force sensor skin, in *IEEE/RSJ International Conference on Intelligent Robots and Systems* (2005), pp. 1818–1823
156. J.-H. Kim, W.-C. Choi, H.-J. Kwon, Development of tactile sensor with functions of contact force and thermal sensing for attachment to intelligent robot finger tip, in *IEEE Sensors*, Daegu, Korea (2006), pp. 1468–1472